NASA TECHNICAL NOTE

NASA TN D-4885

NASA TN D-4885

TECH LIBRARY KAFB, NM

ABSORPTION RATE STICKING PROBABILITIES FOR OXYGEN ON COLUMBIUM AND DILUTE COLUMBIUM-ZIRCONIUM ALLOYS

by Charles A. Barrett

Lewis Research Center
Cleveland, Ohio

NATIONAL AERONAUTICS AND SPACE ADMINISTRATION • WASHINGTON, D. C. • NOVEMBER 1968

ERRATA

NASA Technical Note D-4885

*

ABSORPTION RATE STICKING PROBABILITIES FOR OXYGEN ON

COLUMBIUM AND DILUTE COLUMBIUM-ZIRCONIUM ALLOYS

by Charles A. Barrett

November 1968

Page 31, equation (B-2): The third term on the right side should read

$$-\frac{Q_i T_{2(G)}^{1/2} M^{1/2}}{3.81\, T_0} \sum_{i=2}^{3} \frac{L_i}{D_i^3}$$

Page 32, table VI: The heading for the thirteenth column should read "Total length of ith quartz segments, L, cm."

Page 32, table VI: The following data for specimen 90 should be added at the bottom of the table:

| 90 | 8.78×10^{-6}
4.22×10^{-6}
1.34×10^{-6}
5.72×10^{-7}
2.93×10^{-7}
2.45×10^{-5} | 3.39×10^{-5}
2.16×10^{-5}
4.87×10^{-6}
2.37×10^{-6}
1.06×10^{-6}
1.09×10^{-4} | 313 | 313 | 1253 | 6.35 | 3.10 | 27.75 | 2.76 | 0 | 0 | 34.10 |

ABSORPTION RATE STICKING PROBABILITIES FOR OXYGEN ON

COLUMBIUM AND DILUTE COLUMBIUM-ZIRCONIUM ALLOYS

By Charles A. Barrett

Lewis Research Center
Cleveland, Ohio

NATIONAL AERONAUTICS AND SPACE ADMINISTRATION

ABSTRACT

Sticking probabilities for oxygen on columbium and dilute columbium-zirconium alloys were derived from ratios of oxygen absorption rates to their corresponding oxygen fluxes. Oxygen test pressures were varied from 10^{-7} to 10^{-5} torr over temperatures between 1158 and 1373 K. The absorption rates were derived from a pressure-drop technique and fluxes from constant pressure measurements. The kinetics of the reaction are discussed as well as characteristics of the test method.

ABSORPTION RATE STICKING PROBABILITIES FOR OXYGEN ON COLUMBIUM

AND DILUTE COLUMBIUM-ZIRCONIUM ALLOYS

by Charles A. Barrett

Lewis Research Center

SUMMARY

Reaction rates in oxygen of columbium and dilute columbium-zirconium alloys (up to 0.94 percent Zr) were determined at temperatures between 1158 and 1373 K at times to 236 hours and oxygen pressures between 10^{-7} and 10^{-5} torr. The ratio of these rates to their corresponding oxygen fluxes is the sticking probability. These rates were determined by measurement of a pressure drop across a molecular flow conductance upstream of the pumping specimen. The reaction rates were linear with time and flux and essentially independent of temperature. This indicated that surface adsorption was rate controlling. The rates increased with increasing zirconium content and were considerably lower when the test-chamber wall temperature and specimen temperature were similar (hot-wall case), than when the test-chamber wall was much cooler than the specimen (cold-wall case).

The sticking probabilities derived from a regression analysis of the data were 0.047 and 0.093 for columbium and columbium - 1-percent zirconium in the hot-wall case and 0.077 and 0.15 for columbium and columbium - 1-percent zirconium in the cold-wall case.

A multiple, linear regression analysis of the data shows that the linear absorption rate for dilute columbium-zirconium alloys can be expressed as $\log \overline{R}_i = -1.3326 + 1.000 \log \text{flux} + 0.3028 \text{ wt \% Zr} + 0.2163 X_4$ where $\overline{R}_i$ is the linear absorption rate, flux is the oxygen flux, Zr the weight percent zirconium present in the columbium, and X_4 is the factor which indicates whether the specimen is surrounded by a cold wall (1) or a hot wall (0). The equation explains over 95 percent of the total variability with a standard error of estimate of 0.1414. This equation shows (1) a linear dependence on flux (pressure), (2) no detectable activation energy, (3) a monotonic dependence on zirconium content, and (4) a dependence on whether $X_4 = 1$ for cold-wall conditions or $X_4 = 0$ for hot-wall conditions.

The sticking probabilities and estimating equation are valid until the oxygen solubility is exceeded at the metal surface and columbium monoxide is formed. The time to reach this level can be predicted for any given flux and specimen thickness if the oxygen solubility limit, oxygen diffusion rate, and oxygen sticking probabilities are known.

INTRODUCTION

Columbium and its alloys can take into solution large quantities of oxygen and other interstitial impurities at elevated temperatures. If present in sufficiently large concentrations, these dissolved interstitials tend to degrade the desirable properties of the metal such as resistance to corrosive attack by alkali metals and creep strength at elevated temperatures, which make such alloys of interest for components of advanced space-power systems. This type of contamination would be negligible in space, but is an important consideration in ground testing of components constructed of such alloys. These would be proof tested in laboratory vacuum environments where contaminating molecules are always present.

If it is assumed that oxygen is the most likely serious contaminating gas, then the maximum pickup rate by the alloy as a limiting case is just the number of oxygen molecules colliding with the surface (i.e., flux). For example, calculations based on the Langmuir equation (ref. 1) indicate that an alloy tube with a wall thickness of 0.038 centimeters would reach a level of 2000 ppm oxygen in 9.62 hours at 10^{-5} torr and 96.2 hours for 10^{-6} torr. This is for the gas hitting the outer surface only. This calculation assumes that all the gas in the system is oxygen and that every molecule that hits the surface dissociates and dissolves in the metal, oxygen diffusion being fast enough so that surface flux is rate controlling. However, if the actual partial pressure of oxygen is used in the flux calculation and if only a fraction of the oxygen molecules colliding with the tube surface are adsorbed, the actual time to reach any critical oxygen level would be proportionally longer or the vacuum requirement to reach the critical level would be that much lessened. The ratio of reacting molecules to colliding molecules is termed the sticking probability and is presumed to be a material constant for any alloy.

The purpose of this study was to determine sticking probabilities at temperatures up to 1373 K and oxygen pressures of from 10^{-7} to 10^{-5} torr for pure columbium and the nominal columbium - 1-percent zirconium alloy. Sticking probabilities were determined from oxygen pickup rates run at constant oxygen fluxes at temperatures ranging from 1158 to 1373 K for times up to 240 hours.

In this pressure range the anticipated pickup rates were so small that conventional gravimetric techniques could not be used because they lack the necessary capacity and/or sensitivity for the total specimen weight change involved. Therefore, the rate of pickup was determined by measurement of the pressure drop through a conductance downstream of an oxygen leak, with the pressure over the specimen, which acts as a pump, being constant.

Other investigators who have studied the low-pressure oxygen reactions of columbium or columbium - 1-percent zirconium near 1373 K have run at pressures greater than 10^{-5} torr. Here, absorption takes place for only a short time before surface

scaling begins (refs. 2 to 8). Sticking probabilities can be derived from the early part of the rate curves but are difficult to verify. Pasternak has derived sticking probabilities for oxygen on pure columbium over the pressure and temperature ranges of interest using a chemisorption approach (refs. 9 and 10). The rate data from these studies will be compared with those from this investigation in this report.

The tests were performed at the General Electric Vacuum Laboratory, Schenectady, New York, and are summarized in references 11 and 12. The data and specimens were returned to the NASA Lewis Research Center for analyses and constitute the basis for this report.

The results of the initial phase of this study were published in 1963 (ref. 13); since then, the test procedure and analyses have been revised to incorporate several improvements.

EXPERIMENTAL METHOD, APPARATUS, AND PROCEDURE

The sticking probabilities determined in this study are simply the ratios of two other quantities derived from experimental measurements, namely, the oxygen absorption rate and the corresponding oxygen flux incident on the specimen. The techniques used for determination of these two quantities are described in the following sections, along with a discussion of the experimental uncertainties associated with each of them.

Oxygen Absorption-Rate Measurements

In this study oxygen absorption rates of the test alloys were determined by the pressure-drop technique. This method was originally developed by Wagener for the molecular flow regime (ref. 14) in 1950 and extended by della Porta (refs. 15 and 16) and Orr (ref. 17). The sensitivity of this technique can be of the order of 10^{-11} gram, much beyond the sensitivity of commonly used gravimetric techniques which, at best, are close to 10^{-7} gram (ref. 1). This method is based on the pumping action produced when certain gases are brought into contact with getter materials. The flow of gas being gettered is measured by the magnitude of the pressure drop across a known vacuum conductance. The volumetric gettering or pumping rate Q_i can be expressed by the following equation:

$$Q_i = \Delta P C_o \tag{1}$$

where ΔP is the measured pressure drop through an orifice, capillary, or tube length in the molecular flow range of conductance C_o. The specific rate $\overline{R}_i$ is

3

$$\overline{R}_i = \frac{Q_i K}{A}$$

where K is a conversion factor and A is the specimen area. (More complete definitions of the symbols are presented in appendix A.) In this study the rate $\overline{R}_i$ was determined as a function of temperature, pressure and time.

In order to be able to use the pressure-drop method, it is necessary to assure that the measured pressure drop is attributable only to the pumping action of the specimen. Experimentation verified that this was the situation in our experiments; when no heated specimen was present in the system, there was no detectible pressure-drop across the conductance C_o.

Apparatus

The apparatus for studying continuous oxygen absorption of columbium alloys at low steady-state pressures at temperatures near 1375 K was developed at the General Electric Engineering Laboratory, Schenectady, New York, specifically for this program. Detailed summaries of the apparatus and experimental procedure are given in references 10 and 11.

A photograph of a typical test set-up is shown in figure 1, and a schematic of the essential features of the system is shown in figure 2. The apparatus consists of an orifice throttled, oil-diffusion-pumped system, an oxygen permeation leak between the pump and the test section, a section of known molecular flow conductance, a heated test specimen section, appropriately located vacuum gages, and a mass spectrometer. The system is constructed entirely of borosilicate glass with a quartz test section. The use of an all glass system was necessary in order to avoid extraneous pumping by metal surfaces other than the specimen. It did, however, introduce the possibility of silicon transfer to the test specimen, which would invalidate the measurements. This possibility was checked visually and by mass spectrographic analysis of test specimens for silicon. No evidence of silicon transfer to the test specimens was found. All runs except one were performed with the test section in a resistance-wound tube furnace. The remaining run was induction heated.

The rate of oxygen flow into the test rig was adjusted by varying the temperature of an oxygen permeable silver tube. Generally, once the required temperature was reached, the oxygen leak rate was quite stable and little adjustment was needed throughout a given test. The temperature of the test section was monitored with a calibrated optical pyrometer.
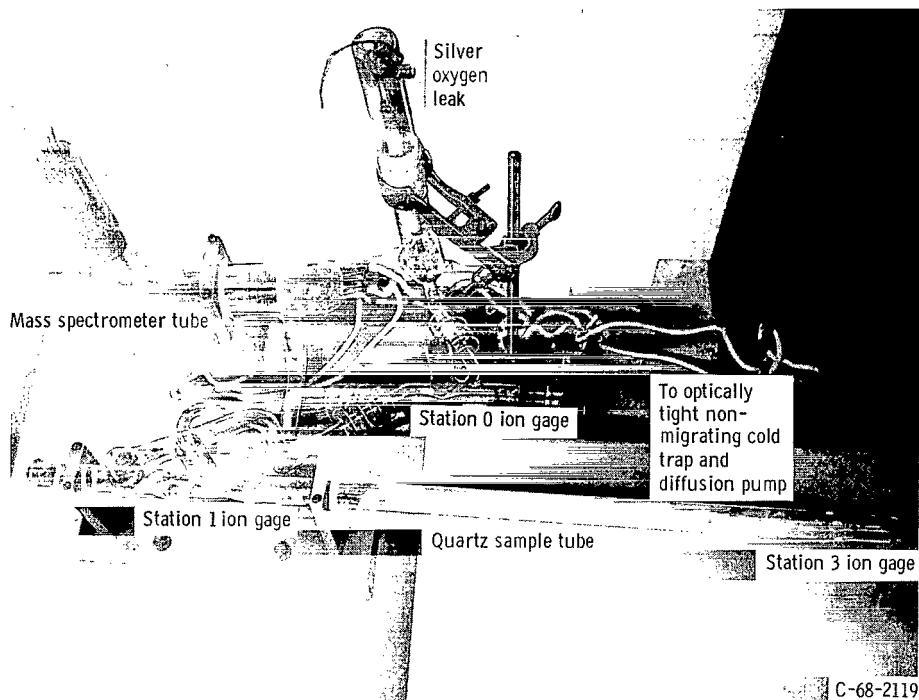
Figure 1. – Low-pressure oxidation rig (scale approximately 1/4).

L   Distance from P_1 gage to beginning of specimen
D_i Inside diameter of test section
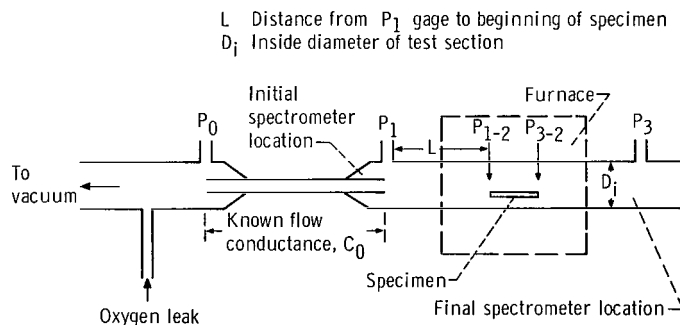
Figure 2. – Oxidation flow conductance test rig.

Pressure measurements were made with miniature Bayard-Alpert thorium dioxide-iridium filament ionization gages with large tubulations and were recorded continuously. The ionization gages were run with reduced emission currents in order to minimize the pumping action of the gages. It was determined experimentally that the pumping action of the vacuum gages and mass spectrometer were negligible compared with the pumping action of the specimen in oxygen. The pressures were measured at three stations, P_0, P_1, and P_3 (fig. 2). For the purpose of this experiment, it is vital that the pressure

5

drop $(P_0 - P_1)$ be accurately measured. Therefore, the individual ionization gages along with their control panels were calibrated in oxygen over the test pressure range of from 10^{-8} to 10^{-4} torr against two secondary-gage standards and were periodically re-calibrated for drift (refs. 11 and 12). The two secondary gages, along with their individual control panels, were calibrated for oxygen in an absolute system. The overall uncertainty in the oxygen pressure estimate for each gage was near 5 percent.

The species of gas present in the system were checked with a calibrated magnetic-deflection mass spectrometer when steady-state conditions were established and at frequent intervals thereafter. In the earlier runs, the mass spectrometer pickup was located near P_1. Later, it was located at P_3 to give a more accurate measure of the gases over the specimen. In order to measure oxygen sticking probabilities accurately, it is necessary that interferences from other species not be significant. At very low pressures, residual gases such as carbon monoxide, water vapor, and hydrogen may constitute an unacceptably large fraction of the gases present. Therefore, for deter-minations of oxygen sticking probabilities, it was arbitrarily decided to discard any set of data for which the mass spectrometer data indicated an oxygen concentration less than 85 percent over the specimen. In this concentration range (100 to 85 percent) the overall scatter in the data was not a function of the oxygen percentage (see appendix B).

Test Specimens

A description of the individual test specimens is given in table I. They were all sized to have a total surface area of approximately 20 square centimeters and were cut from sheets of several thicknesses that ranged in size from 0.076 to 0.127 centimeter. The as-received sheet were
   (1) Vapor degreased in trichloroethylene
   (2) Sonically cleaned in detergent
   (3) Rinsed in tap water and then in distilled water
   (4) Lightly etched in 55-percent water - 25-percent nitric acid - 20-percent hydro-
       fluoric acid (3 to 5 sec)
   (5) Rinsed in distilled water and air dried in an oven at 43° C (110° F)
Early specimens were 1.27 wide by 7.62 centimeters long; later specimens were ap-proximately 2.54 wide by 3.81 or 4.44 centimeters long. The shorter, wider specimen tended to give a smaller pressure gradient along its length and rested nearer the center plane of the test section than the longer narrower specimen. The derived rate data from either size did not show any detectable difference, however. The surface finish of each specimen is listed in table I.

The tests were performed in three different test rigs which are described in refer-

TABLE I. - TEST SPECIMEN

[Nominal alloy composition, columbium - 1 wt % zirconium.]

(a) As-received

Specimen	Thickness, cm	Initial chemistry, ppm by weight				Surface finish, μcm	Sample
		Oxygen	Nitrogen	Carbon	Hydrogen		
Columbium - 0.75 wt % zirconium	0.127	930	180	20	4	152.4	50, 36, 37, 88
Columbium - 0.89 wt % zirconium	.114	360	23	48	6	106.7	90
Columbium - 0.94 wt % zirconium	.076	30	64	27	1	38.1	59, 61
Pure columbium	.076	210	41	16	6.7	30.5	52, 51
Pure columbium	.114	92	55	32	3	53.3	3

(b) Treated

Sample	Dimensions, cm	Surface area, cm	Final weight, g	Final oxygen content, ppm by weight	Number of analyses	Conductance, liter/sec
3	1.298 by 7.640	21.88	9.56671	15 900	11	0.615
36	1.275 by 7.625	21.77	10.72576	3 040	10	.615
37	1.290 by 7.625	21.93	10.51443	3 250	10	.615
50	2.062 by 4.463	20.10	10.16088	2 220	8	.615
51	2.050 by 4.458	19.26	5.58592	254	7	.536
52	2.050 by 4.443	19.20	5.61180	5 077	6	.615
59	2.672 by 3.815	21.35	6.53260	3 600	10	.595
61	2.672 by 3.815	21.37	6.60003	7 690	12	.646
88	2.436 by 3.802	20.11	10.17256	5 520	6	.619
90	2.451 by 3.810	20.11	9.03159	3 330	7	.538

ences 10 and 11. Their major differences were in the diameter of the test section and in the size and position of the conductance tube. The value for this conductance C_o at its approximate temperature during each test is also listed in table I.

Procedure

A test specimen, previously cleaned and weighed to the nearest 0.01 milligram, was placed in the apparatus at the end of the test section. The system was sealed, evacuated, and outgassed at 723 K overnight. The quartz test section was then heated to the test temperature and further outgassed until a pressure in the 10^{-8} torr region or lower was obtained. The specimen was magnetically pushed into the center of the test

TABLE II. – EXPERIMENTAL CONDITIONS AND TEST RESULTS FOR OXYGEN ABSORPTION STUDIES

Specimen	Time, hr	Temperature at test specimen, $T_{2(s)}$, K	Observed oxygen pressures, torr			Oxygen pickup rate over test interval, (g/cm^2)/hr		Accumulative weight gain over test interval, W_p/A, g/cm^2	Oxygen content, percent	Derived oxygen pressures, torr			Oxygen flux, F, (g/cm^2)/hr	Sticking probability, ϵ
			$\bar{P}_0$	$\bar{P}_1$	$\bar{P}_3$	$\bar{R}_i$	$\sigma\bar{R}_i$			$\bar{P}_{1-2}$	$\bar{P}_{3-2}$	$\bar{P}_2$		
3	0 to 20	1200	2.30×10^{-4}	4.79×10^{-5}	----------	3.20×10^{-5}	0.425×10^{-5}	6.36×10^{-4}	[c]99.7	----------	----------	----------	----------	------
	21 to 235	1200	2.29×10^{-4}	6.00×10^{-5}	----------	2.98×10^{-5}	1.214×10^{-5}	6.35×10^{-3}	99.73	----------	----------	----------	----------	------
	0 to 235	1200	2.30×10^{-4}	5.90×10^{-5}	----------	2.99×10^{-5}	1.176×10^{-5}	7.04×10^{-3}	99.73	----------	----------	----------	----------	------
36	21	1253	1.03×10^{-5}	1.65×10^{-6}	1.76×10^{-7}	1.53×10^{-6}	0.131×10^{-6}	3.19×10^{-5}	[c]99.7	1.26×10^{-6}	3.62×10^{-7}	6.75×10^{-7}	2.27×10^{-5}	0.0675
	19	1253	7.10×10^{-5}	1.35×10^{-5}	1.44×10^{-6}	1.01×10^{-5}	$.210\times10^{-5}$	1.96×10^{-4}	-----	1.36×10^{-5}	2.96×10^{-6}	6.34×10^{-6}	2.13×10^{-4}	.0475
	24	1373	9.31×10^{-6}	1.59×10^{-6}	1.39×10^{-7}	1.36×10^{-6}	$.048\times10^{-6}$	3.27×10^{-5}	99.7	1.42×10^{-6}	2.99×10^{-7}	6.52×10^{-7}	2.09×10^{-5}	.0651
	23	↓	9.09×10^{-5}	1.53×10^{-5}	9.10×10^{-7}	1.33×10^{-5}	$.094\times10^{-5}$	3.07×10^{-4}	99.9	1.34×10^{-5}	1.96×10^{-6}	5.12×10^{-6}	1.64×10^{-4}	.0810
	21		4.27×10^{-5}	6.35×10^{-6}	5.13×10^{-7}	6.41×10^{-6}	$.348\times10^{-6}$	1.35×10^{-4}	99.9	4.25×10^{-6}	1.10×10^{-6}	2.16×10^{-6}	6.93×10^{-5}	.0925
	21	↓	3.35×10^{-6}	5.85×10^{-7}	7.80×10^{-8}	4.88×10^{-7}	$.493\times10^{-7}$	1.03×10^{-5}	99.4	5.44×10^{-7}	1.68×10^{-7}	3.02×10^{-7}	9.69×10^{-6}	.0525
37	23	1253	5.00×10^{-6}	8.56×10^{-7}	1.12×10^{-7}	7.25×10^{-7}	0.436×10^{-7}	1.66×10^{-5}	[c]99.4	7.36×10^{-7}	2.30×10^{-7}	4.11×10^{-7}	1.38×10^{-5}	0.0525
	72		8.74×10^{-6}	1.05×10^{-6}	[b]1.64×10^{-7}	1.35×10^{-6}	$.140\times10^{-6}$	9.68×10^{-5}	99.7	2.58×10^{-7}	2.37×10^{-7}	2.47×10^{-7}	8.29×10^{-6}	.163
	21	↓	2.54×10^{-5}	3.61×10^{-6}	3.88×10^{-7}	3.81×10^{-6}	$.315\times10^{-6}$	7.97×10^{-5}	99.8	2.04×10^{-6}	7.98×10^{-7}	1.28×10^{-6}	4.28×10^{-5}	.0890
	24		5.31×10^{-5}	8.14×10^{-6}	7.76×10^{-7}	7.87×10^{-6}	$.281\times10^{-6}$	1.89×10^{-4}	99.8	5.61×10^{-6}	1.60×10^{-6}	3.00×10^{-6}	1.00×10^{-4}	.0783
	22		9.01×10^{-5}	1.23×10^{-5}	1.27×10^{-6}	1.36×10^{-5}	$.045\times10^{-5}$	3.00×10^{-4}	99.9	6.08×10^{-6}	2.61×10^{-6}	3.98×10^{-6}	1.34×10^{-4}	.102
	6.5	↓	2.42×10^{-4}	3.38×10^{-5}	3.58×10^{-6}	3.72×10^{-5}	$.196\times10^{-5}$	2.42×10^{-4}	-----	1.43×10^{-5}	7.37×10^{-6}	1.03×10^{-5}	3.44×10^{-4}	.108
50	23	1253	8.81×10^{-6}	1.36×10^{-6}	[a]2.33×10^{-7}	1.42×10^{-6}	0.066×10^{-6}	3.27×10^{-5}	[c]99.3	7.62×10^{-7}	4.79×10^{-7}	6.04×10^{-7}	2.03×10^{-5}	0.0701
	24	1373	1.15×10^{-5}	1.75×10^{-6}	2.55×10^{-5}	1.86×10^{-6}	$.175\times10^{-6}$	4.50×10^{-5}	98.9	9.76×10^{-7}	5.49×10^{-7}	7.32×10^{-7}	2.35×10^{-5}	.0793
	21	1373	8.26×10^{-5}	1.32×10^{-5}	1.02×10^{-6}	1.33×10^{-5}	$.061\times10^{-5}$	2.79×10^{-4}	99.8	8.55×10^{-6}	2.20×10^{-6}	4.34×10^{-6}	1.39×10^{-4}	.0957
	23	1253	8.16×10^{-5}	1.31×10^{-5}	1.26×10^{-6}	1.31×10^{-5}	$.049\times10^{-5}$	3.00×10^{-4}	99.8	8.23×10^{-6}	2.59×10^{-6}	4.62×10^{-6}	1.55×10^{-4}	.0846
51	236	1253	5.61×10^{-7}	9.39×10^{-8}	2.91×10^{-8}	7.72×10^{-8}	0.774×10^{-8}	1.82×10^{-5}	[d]91.3	1.20×10^{-7}	5.84×10^{-8}	8.37×10^{-8}	2.81×10^{-6}	0.0275
52	23	1408	3.50×10^{-6}	[f]6.15×10^{-7}	1.66×10^{-7}	5.75×10^{-7}	0.295×10^{-5}	1.32×10^{-5}	[c]94.4	5.31×10^{-7}	3.62×10^{-7}	4.38×10^{-7}	1.39×10^{-5}	0.0415
	[e]72	1408	7.92×10^{-6}	1.41×10^{-6}	3.21×10^{-7}	1.30×10^{-6}	$.063\times10^{-6}$	9.37×10^{-5}	-----	1.24×10^{-6}	7.00×10^{-7}	9.32×10^{-7}	2.95×10^{-5}	.0441
	22	1373	3.88×10^{-5}	5.87×10^{-6}	1.06×10^{-6}	6.57×10^{-6}	$.510\times10^{-6}$	1.44×10^{-4}	-----	3.47×10^{-6}	2.28×10^{-6}	2.81×10^{-6}	9.01×10^{-5}	.0729
	23	1373	9.08×10^{-5}	1.38×10^{-5}	2.38×10^{-6}	1.54×10^{-5}	$.111\times10^{-5}$	3.55×10^{-4}	-----	8.30×10^{-6}	5.13×10^{-6}	6.53×10^{-6}	2.09×10^{-4}	.0737
	22	1253	2.86×10^{-6}	5.67×10^{-7}	1.82×10^{-7}	4.59×10^{-7}	$.359\times10^{-7}$	1.01×10^{-5}	95.6	5.58×10^{-7}	3.74×10^{-7}	4.57×10^{-7}	1.53×10^{-5}	.0300
	69		7.19×10^{-6}	1.29×10^{-6}	3.58×10^{-7}	1.18×10^{-6}	$.126\times10^{-6}$	8.14×10^{-5}	98.4	1.09×10^{-7}	7.37×10^{-7}	8.96×10^{-7}	3.01×10^{-5}	.0393
	23		3.68×10^{-5}	6.13×10^{-6}	1.40×10^{-6}	6.13×10^{-6}	$.664\times10^{-6}$	1.40×10^{-4}	99.0	4.45×10^{-6}	2.88×10^{-6}	3.58×10^{-6}	1.20×10^{-4}	.0511
	22	↓	9.08×10^{-5}	1.42×10^{-5}	2.92×10^{-6}	1.53×10^{-5}	$.160\times10^{-5}$	3.37×10^{-4}	97.7	8.88×10^{-6}	6.01×10^{-6}	7.31×10^{-6}	2.45×10^{-4}	.0624

59	93 to 178	1373	8.87×10^{-6}	1.37×10^{-6}	1.15×10^{-7}	1.20×10^{-6}	0.055×10^{-6}	1.02×10^{-4}	[d]89.4	2.11×10^{-6}	2.37×10^{-7}	7.07×10^{-7}	2.27×10^{-5}	0.0530
	190 to 231	1373	8.30×10^{-6}	1.39×10^{-6}	1.22×10^{-7}	1.10×10^{-6}	$.066 \times 10^{-6}$	4.48×10^{-5}	89.4	2.20×10^{-6}	2.51×10^{-7}	7.43×10^{-7}	2.38×10^{-5}	$.0462$
61	19	1158	1.40×10^{-5}	1.17×10^{-6}	2.36×10^{-7}	2.20×10^{-6}	0.151×10^{-6}	4.20×10^{-5}	[d]92.1	9.91×10^{-7}	4.46×10^{-7}	6.65×10^{-7}	2.32×10^{-5}	0.0949
	24	1253	1.43×10^{-5}	1.23×10^{-6}	2.19×10^{-7}	2.25×10^{-6}	$.100 \times 10^{-6}$	5.41×10^{-5}	-----	1.13×10^{-6}	4.31×10^{-7}	6.98×10^{-7}	2.34×10^{-5}	$.0961$
	21	1373	1.42×10^{-5}	1.20×10^{-6}	2.44×10^{-7}	2.24×10^{-6}	$.135 \times 10^{-6}$	4.71×10^{-5}	86.4	1.12×10^{-6}	5.02×10^{-7}	7.50×10^{-7}	2.40×10^{-5}	$.0932$
	24	1373	2.11×10^{-4}	1.44×10^{-5}	2.09×10^{-6}	3.39×10^{-5}	$.224 \times 10^{-5}$	8.16×10^{-4}	-----	9.28×10^{-6}	3.54×10^{-6}	5.73×10^{-6}	1.84×10^{-4}	$.185$
	23	1253	1.80×10^{-4}	1.36×10^{-5}	3.04×10^{-6}	2.87×10^{-5}	$.116 \times 10^{-5}$	6.59×10^{-4}	-----	1.04×10^{-5}	4.90×10^{-6}	7.14×10^{-6}	2.39×10^{-4}	$.120$
	21	1158	1.79×10^{-4}	1.41×10^{-5}	3.22×10^{-6}	2.85×10^{-5}	$.100 \times 10^{-5}$	5.99×10^{-4}	-----	1.09×10^{-5}	4.97×10^{-6}	7.36×10^{-6}	2.57×10^{-4}	$.111$
88	22	1253	2.32×10^{-4}	1.63×10^{-5}	2.09×10^{-6}	4.12×10^{-5}	0.248×10^{-5}	9.07×10^{-4}	[d]95.1	5.95×10^{-6}	2.09×10^{-6}	3.53×10^{-6}	2.43×10^{-4}	0.170
	18	↓	1.02×10^{-4}	7.33×10^{-6}	8.76×10^{-7}	1.81×10^{-5}	$.022 \times 10^{-5}$	3.26×10^{-4}	97.7	2.80×10^{-6}	8.76×10^{-7}	1.57×10^{-6}	1.08×10^{-4}	$.168$
	20		2.36×10^{-5}	1.67×10^{-6}	2.42×10^{-7}	4.19×10^{-6}	$.162 \times 10^{-6}$	8.36×10^{-5}	92.7	6.20×10^{-7}	2.42×10^{-7}	3.87×10^{-7}	2.66×10^{-4}	$.157$
	16		9.79×10^{-6}	7.62×10^{-7}	1.25×10^{-7}	1.72×10^{-6}	$.015 \times 10^{-6}$	2.76×10^{-5}	88.4	3.30×10^{-7}	1.25×10^{-7}	2.03×10^{-7}	1.40×10^{-5}	$.123$
	27	1158	2.06×10^{-4}	1.57×10^{-5}	3.06×10^{-6}	3.64×10^{-5}	$.589 \times 10^{-5}$	9.89×10^{-4}	92.7	6.59×10^{-6}	3.43×10^{-6}	4.75×10^{-6}	3.27×10^{-4}	$.111$
	16	1158	8.84×10^{-5}	7.06×10^{-6}	1.52×10^{-6}	1.55×10^{-5}	$.016 \times 10^{-5}$	2.48×10^{-4}	92.7	3.18×10^{-6}	1.52×10^{-6}	2.20×10^{-6}	1.51×10^{-4}	$.103$
	23	1158	2.17×10^{-5}	1.74×10^{-6}	4.39×10^{-7}	3.81×10^{-6}	$.088 \times 10^{-6}$	8.75×10^{-5}	90.6	7.82×10^{-7}	4.39×10^{-7}	5.86×10^{-7}	4.03×10^{-5}	$.0945$
90	24	1253	7.17×10^{-5}	8.78×10^{-6}	7.95×10^{-7}	9.94×10^{-6}	1.37×10^{-6}	2.39×10^{-4}	[d]97.1	8.34×10^{-6}	1.59×10^{-6}	3.64×10^{-6}	1.22×10^{-4}	0.0814
	23		4.44×10^{-5}	4.22×10^{-6}	4.84×10^{-7}	6.35×10^{-6}	$.608 \times 10^{-6}$	1.46×10^{-4}	97.7	2.56×10^{-6}	9.68×10^{-7}	1.57×10^{-6}	5.28×10^{-5}	$.120$
	20		[a]1.04×10^{-5}	1.34×10^{-6}	1.28×10^{-7}	1.43×10^{-6}	----------	2.72×10^{-5}	90.8	1.35×10^{-6}	2.56×10^{-7}	5.88×10^{-7}	1.97×10^{-5}	$.0725$
	24		4.97×10^{-6}	5.72×10^{-7}	7.90×10^{-8}	6.94×10^{-7}	$.285 \times 10^{-7}$	1.66×10^{-5}	92.2	4.99×10^{-7}	1.58×10^{-7}	2.81×10^{-7}	9.42×10^{-6}	$.0737$
	22		2.27×10^{-6}	2.93×10^{-7}	4.28×10^{-8}	3.12×10^{-7}	$.335 \times 10^{-7}$	6.88×10^{-6}	93.8	2.98×10^{-7}	8.56×10^{-8}	1.60×10^{-7}	5.36×10^{-6}	$.0582$
	22		2.27×10^{-4}	2.45×10^{-5}	2.35×10^{-6}	3.20×10^{-5}	$.233 \times 10^{-5}$	7.07×10^{-4}	99.3	1.94×10^{-5}	4.70×10^{-6}	9.55×10^{-6}	3.20×10^{-4}	$.100$

[a]Steady-state value.

[b]$\bar{P}_3$ gage off for 20 hr; P_3 estimated from P_0 and P_1 gages.

[c]Mass spectrometer between P_0 and P_1 gages.

[d]Mass spectrometer at P_3 gage.

[e]Rate constant ($\bar{R}_i$) derived from last 6 hr of data because of gage recorder failure.

[f]Power off P_1 gage for 10 hr; P_1 estimated from P_0 and P_3 gages.

section where it rested in a horizontal position with its edges supported by the quartz test section walls. The specimen was outgassed until the system pressure dropped close to what it was prior to the introduction of the specimen. This sometimes required up to three days of pumping. At this time the oxygen leak was activated.

After the oxygen leak was activated, it typically took a few minutes for P_1 to rise to 1×10^{-6} torr and for a constant pressure difference, for $(P_0 - P_1)$, to be obtained. Zero time was taken when P_1 reached the designated test pressure.

At the end of the test period, the power to the silver leak heater was shut off as well as the power to the specimen heater. Shortly thereafter P_1 dropped to below 1×10^{-7} torr and no significant pressure difference was observed between P_0, P_1, and P_3.

After the apparatus had cooled to room temperature, it was backfilled with nitrogen, it was opened, and the specimen was removed. The specimen was reweighed, sectioned, and analyzed for oxygen by the vacuum fusion technique. Selected sections of the specimen were mounted for metallography and microhardness determinations. In cases where there was apparent surface oxidation, X-ray diffraction techniques were used to identify the surface oxides.

In some of the tests specimens (3, 59, and 51) the temperature and pressure conditions were maintained constant throughout the entire run. In the other tests, designated as step runs, pressure and temperature conditions were successively varied stepwise, with the same specimen. On each step change the conditions were held constant long enough to allow steady-state measurements to be taken.

Test times, specimen dimensions, surface area, average temperature, and average pressures over the test period of the specimen are summarized in tables I and II.

Besides test times and temperature, the observed data include test pressures at P_0, P_1, and P_3. These were recorded continuously and were arbitrarily listed for every hour. These values were then converted to oxygen pressures from the calibration values. The averages of these converted values are listed in table II for a given test temperature and time interval.

Also listed in table II, wherever possible, is the percent oxygen based on at least one mass spectrometer scan. The location of the mass spectrometer and the number scans that were averaged is also indicated.

RESULTS

Determination of Oxygen Absorption Rates and Estimated Accuracy of Determinations

The gettering rate at any time can be calculated from the relation

$$R_i = \frac{(P_0 - P_1)C_0 K}{A} \tag{2}$$

Here, P_0 and P_1 are oxygen pressures, C_0 is the conductance between the two pressures, K is a conversion factor based on the ideal gas law to give grams per hour, and A is the area of the test specimen. The average rate for a given time interval can be found by substituting average pressures in equation (2). The average value for each test interval $\overline{R}_i$ is listed in table II. This value was actually determined for each hour of the test interval in order to derive the standard deviation as well as the average value. The standard deviation divided by the average value gives the coefficient of variation $m\overline{R}_i$, which is a measure of the variability of $\overline{R}_i$ over the test interval.

During any given step or run, once test conditions were set they held quite steady. This is indicated by the low coefficient of variation on the rate constants which overall averaged just under 7 percent, based on the hourly values.

It is clear from equation (2) that the accuracy of the oxygen absorption rate determinations is strongly dependent on the accuracy with which the conductance C_0 between the gages at P_0 and P_1 is known and on the accuracy of measurement of the pressure drop between these two stations $(P_0 - P_1)$, as well as on an accurate knowledge of the specimen area. For the two later test setups, used for the greater part of this study, the conductance could be calculated in a straightforward way (ref. 18) and is believed to be known to an accuracy of about 1 percent. In the first rig (ref. 11), the conductance was experimentally calibrated due to its irregular geometry and is believed to be accurate to about 1.5 percent.

The accuracy of the pressure drop term $(P_0 - P_1)$ depends on how good and stable the oxygen sensitivity corrections are for each gage. The uncertainty associated with each oxygen pressure measurement was estimated as being close to 5 percent.

The specimen area term in the denominator of equation (2) is simply the geometric area of the specimens. From conventional dimensional measurements, this term is known with an uncertainty of about 0.4 percent. From these uncertainties an error analysis gave an overall uncertainty of close to 7 percent for the oxygen absorption rate.

Accumulative Weight Gains

From the successive hourly R_i values within a test interval, the accumulative weight gain is:

$$W_{p/A} = \sum_{i=0}^{i=n-1} \frac{R_i + R_{i+1}}{2} \Delta t \tag{3}$$

where n is the last incremental hour time point and Δt is the time interval. The W_p values are listed in table II. If W_p values for time intervals of 1 hour are plotted against time on a log-log plot for each test run (or step), typical accumulated weight-gain curves like those found in the oxidation literature result. Several such curves are shown in figure 3.
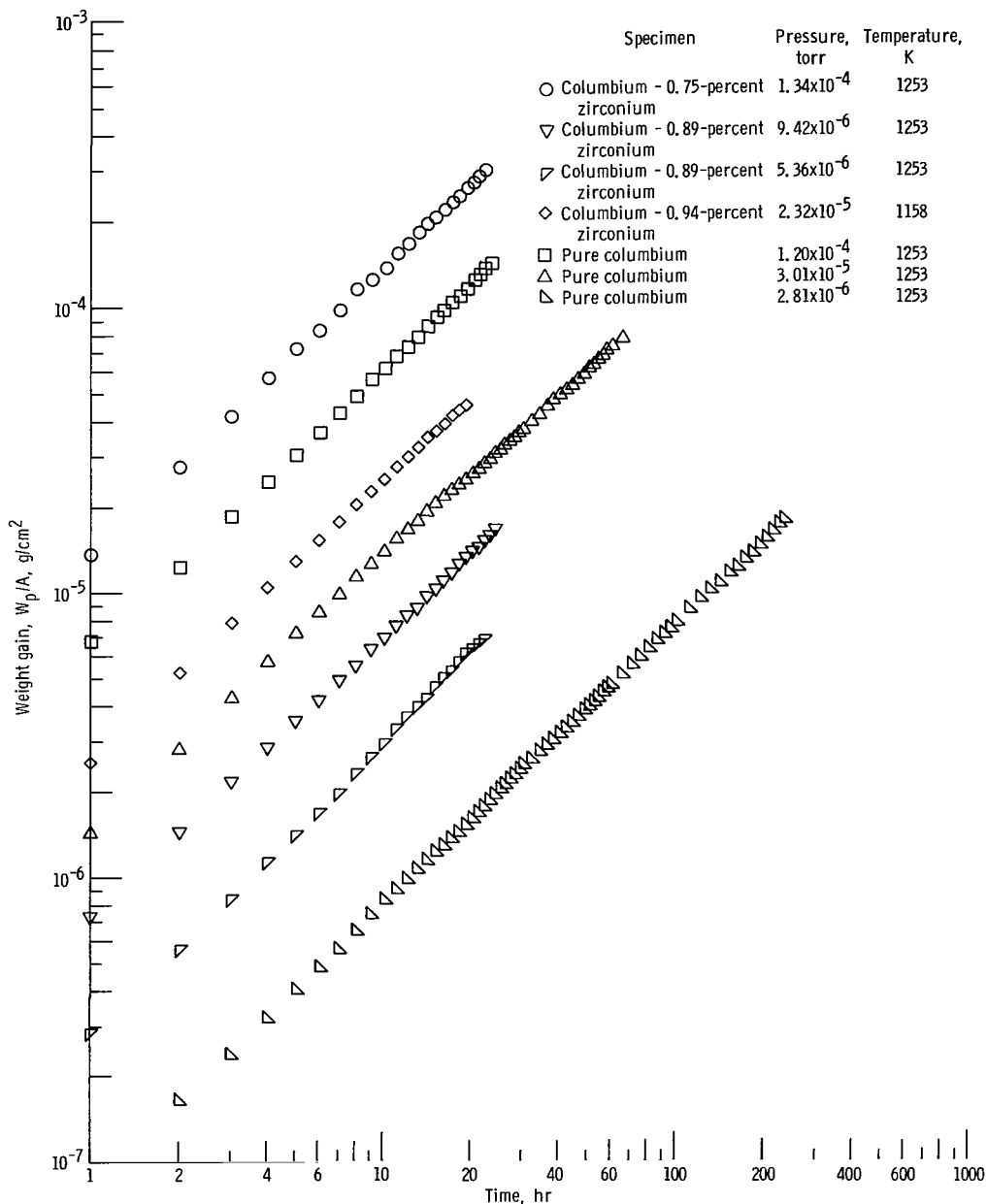
	Specimen	Pressure, torr	Temperature, K
○	Columbium - 0.75-percent zirconium	1.34×10^{-4}	1253
▽	Columbium - 0.89-percent zirconium	9.42×10^{-6}	1253
▽	Columbium - 0.89-percent zirconium	5.36×10^{-6}	1253
◇	Columbium - 0.94-percent zirconium	2.32×10^{-5}	1158
□	Pure columbium	1.20×10^{-4}	1253
△	Pure columbium	3.01×10^{-5}	1253
◁	Pure columbium	2.81×10^{-6}	1253

Figure 3. - Oxygen weight gain for various columbium and dilute columbium-zirconium alloys as function of time, average oxygen flux, and specimen temperature. Weight is nearly linear with time and increases with increasing flux for a given alloy.

Experimental Verification of the Accuracy of Calculated Oxygen Absorption Rates

As described in the preceding section, the accumulative weight gain of a gettering specimen exposed to oxygen at high temperatures over a prolonged time period may be predicted from a knowledge of the oxygen absorption rates over suitable time intervals. The accuracy of the prediction and thus of the method involved may be experimentally verified by determining the weight change resulting from the high-temperature exposure, assuming that the total weight change is due to absorption of oxygen. The validity of this assumption can be ascertained by chemical analysis of the specimen.

Such a comparison of the predicted accumulative weight gains, based on determinations of the oxygen absorption rates as described previously, with the weight gain determined by weighing the specimen before and after test and finally with the amount of oxygen increase during the test as determined by vacuum fusion analysis is shown in table III. Analysis of variance of the data in table III showed no significant difference in the values derived by the three different methods. Over the range of total weight gains studied the values agree to within 5 percent. This agreement is considered excellent and verifies the accuracy of the experimental method for the determination of oxygen absorption rates at low oxygen pressures. (This method can also be used in the controlled doping of oxygen (or other reactive gases) for selected metal alloys at elevated temperatures. See ref. 19.)

There was some uncertainty as to whether the long period of outgassing at the test temperature just prior to starting the oxygen leak changed the initial specimen weight and oxygen chemistry significantly which, in turn, would affect the ΔW_g and ΔW_c

TABLE III. - OVERALL WEIGHT GAIN ESTIMATES

FOR TEST SPECIMENS

Specimen	Weight gain, g		
	By weight change, ΔW_g	By oxygen analysis, ΔW_c	By pressure drop, ΔW_p
3	0.15299	0.15133	0.15375
36	.01918	.02264	.01659
37	.02372	.02438	.02069
50	.01710	.01304	.01454
51	.00071	.00024	.00035
52	.02633	.02731	.02350
59	.02104	.02203	-------
61	.04381	.04924	.05031
88	.04768	.04664	.05385
90	.02820	.02676	.02435

values listed in table III. In order to evaluate this possibility, an 0.127 centimeter thick columbium columbium - 0.75-percent zirconium sample was outgassed for 20 hours after the usual baking out of the system and then removed from the rig prior to testing. The pressure dropped from 10^{-4} torr initially to the mid 10^{-8} torr range after 20 hours. There was no detectable change in weight or oxygen chemistry of the specimen.

Oxygen Flux Over Specimen

In the preceding sections, it was shown that the rate of oxygen absorption at low pressures can be measured with high accuracy for gettering materials like columbium and columbium - 1-percent zirconium by use of the pressure-drop technique. In order to determine sticking probabilities, it is also necessary to know the corresponding oxygen flux incident on the specimen. This quantity was derived from the free molecular flow expression (ref. 1)

$$F = 209.88\ \overline{P}_2 \left(\frac{M}{T_{2(G)}}\right)^{1/2} \tag{4}$$

where F is the oxygen flux, $T_{2(G)}$ is the absolute temperature characteristic of the oxygen molecules in the test region, M is the molecular weight of oxygen, and $\overline{P}_2$ is an estimate of the oxygen pressure over the specimen. Flux values for the experiments previously described are shown in table II.

Unfortunately, for the experimental arrangement used in this type of experiment the flux cannot be determined with the same high certainty as the rate of oxygen absorption. This stems primarily from the uncertainty regarding the value to assign to $\overline{P}_2$. An estimate of the temperature of the molecules $T_{2(G)}$ is also difficult to estimate, but fortuitously, regardless of its value it cancels out because it is also used in the derivation of $\overline{P}_2$. This estimate of $\overline{P}_2$ is derived from both $\overline{P}_1$ and $\overline{P}_3$ and is discussed in detail in appendix B. The uncertainty in this estimate of $\overline{P}_2$ was on the order of 12 percent. The uncertainty in the flux measurement is difficult to estimate directly. If equation (4) is assumed and an exponential drop in pressure along the specimen length is reasonable, with the temperature of the molecules essentially cancelled out, then a 12-percent uncertainty can be expected.

Determination of Sticking Probabilities

The ratio of the oxygen absorption rate R_i to its corresponding flux (average or

instantaneous) can be thought of as the pumping efficiency or, in terms of equilibrium chemisorption theory, as the steady-state sticking probability (i. e. , the fraction of impinging molecules that actually stick to and react with the metal surface). The uncertainty in this estimate, based on the uncertainties in $\overline{R}_i$ and F was calculated to be about 13 percent derived from the individual values of the absorption rates and fluxes shown in table II.

Sticking probabilities derived from multiple regression analysis of the data have considerable utility because they can be estimated for various levels of the significant variables along with their upper and lower standard deviation limits. This method also indicates which factors were not significant. Table IV lists these derived sticking probabilities at selected levels of the significant variables along with their error limits. These values were constant over the flux range and independent of temperature over the range studied (1158 to 1373 K). They are strictly a function of the zirconium content in the columbium and whether the tests were hot walled or cold walled. They range from approximately 0.05 for pure columbium to 0.09 for the columbium - 1-percent-zirconium alloy for the hot-wall case. For the cold-wall case these values are increased to 0.08 for pure columbium and 0.15 for the columbium - 1-percent-zirconium alloy.

TABLE IV. - STICKING PROBABILITIES DERIVED FROM REGRESSING EQUATIONS WITH

UPPER AND LOWER ONE SIGMA VALUES

[Number of data points included in regression analysis, 46; b_1 = 1.000.]

Temperature effect	Hot-wall case, $X_4 = 0$				Cold-wall case, $X_4 = 1$				Standard deviation
	Columbium		Columbium - 1-percent zirconium		Columbium		Columbium - 1-percent zirconium		
	Temperature, K								
	1158	1373	1158	1373	1158	1373	1158	1373	
	Sticking probabilities								
Included	0.0617	0.0656	0.125	0.133	0.104	0.110	0.210	0.224	+1 sigma
	.0444	.0472	.0900	.0957	.0747	.0794	.151	.161	
	.0319	.0340	.0648	.0689	.0537	.0571	.109	.116	-1 sigma
Excluded	0.0644		0.129		0.106		0.212		+1 sigma
	.0465		.0934		.0765		.154		
	.0336		.0674		.0552		.111		-1 sigma

Regression Analysis of Rate Data

Separate log-log plots were made for pure columbium and the nominal columbium - 1-percent-zirconium alloy of the linear rate constants $\overline{R}_i$ against their respective fluxes for each test condition. These are shown in figures 4 and 5 for the furnace-heated specimens. Specimen 88 was induction heated; data for this run are plotted separately on figure 6. The temperature of each test is indicated also. Although there is a fairly broad scatter band, the data points seem to fall on nearly straight lines with a slope of near unity. The maximum possible value for sticking probabilities is unity (i.e., $\overline{R}_i$ = flux). A line representing this line is also plotted in each of the figures.

A simple linear regression was run for the data on each plot following the model

$$\log \overline{R}_i = a + b_1 \log flux \tag{5}$$
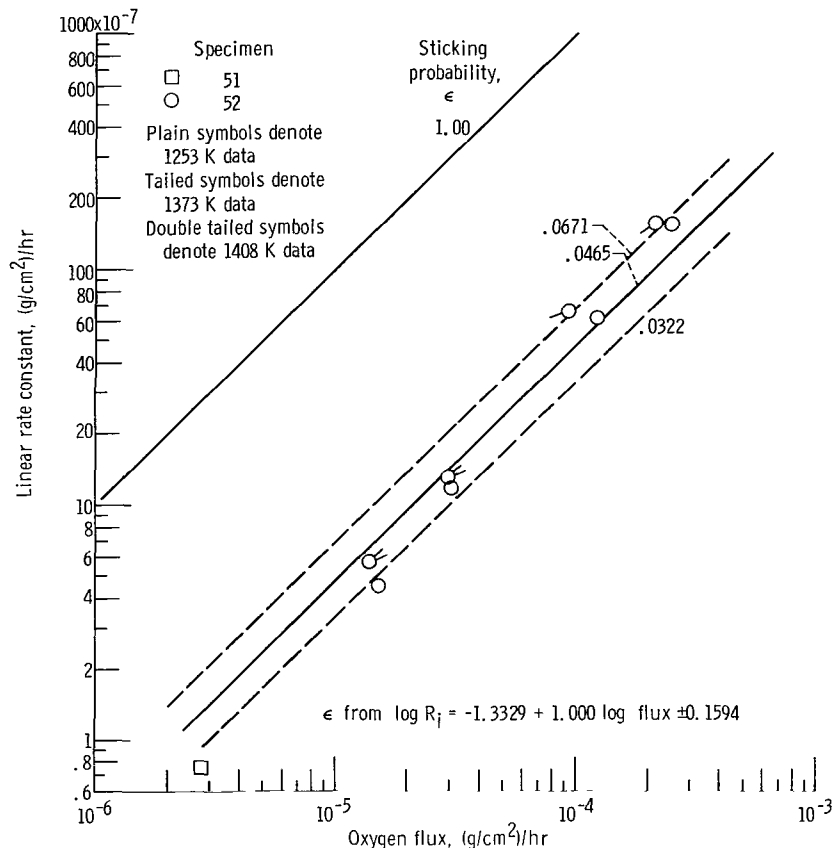
Figure 4. - Linear oxygen absorption of pure columbium as function of oxygen flux and specimen temperature for hot-wall case. Diagonal lines indicate range of sticking probabilities from regression equation. The regression line is derived from nine data points.
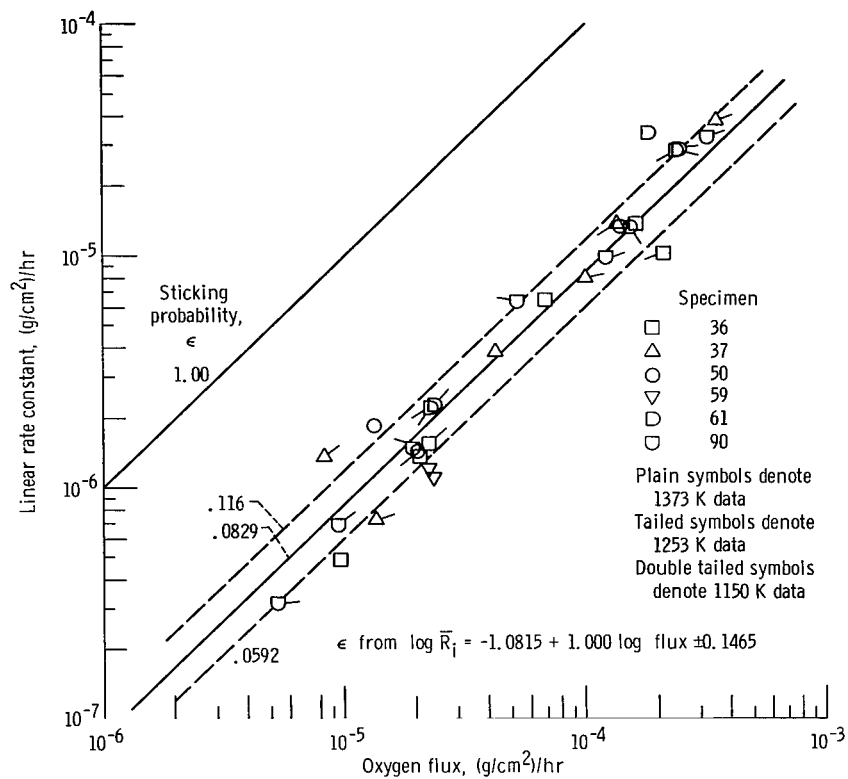
Figure 5. – Linear oxygen absorption of dilute columbium-zirconium for hot-wall case. Diagonal lines indicate range of sticking probabilities from regression equation. The regression line is derived from 30 data points.

17
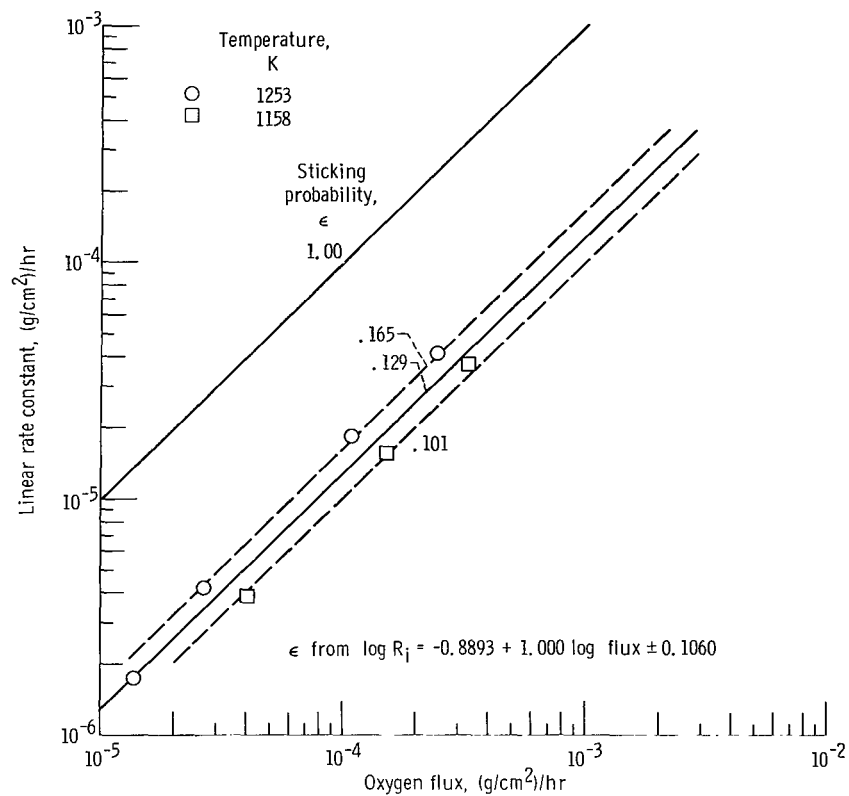
Figure 6. – Linear oxygen absorption of columbium – 0.75-percent zirconium as function of oxygen flux and specimen temperature for cold-wall case. Diagonal lines indicate range of sticking probabilities from regression equation. The regression line is derived from seven data points.

TABLE V. - LINEAR REGRESSION VALUES: $Y = a + b_1X_1 + b_2X_2 + b_3X_3 + b_4X_4$

[Y = log Ri; X = log flux; $X_2 = 1/T_s$; X_3 = wt % Zr; X_4 = hot or cold wall.]

Number of data points included, n	Conditions	Y-intercept, a	Partial regression coefficients			Activation energy (a)				Partial regression coefficients				Fraction of total variation, R^2	Standard error estimate (b)
			b_1	Sigma b_1	b_2	E_a cal	E_a J	Sigma E_a cal	Sigma E_a J	b_3	Sigma b_3	b_4	Sigma b_4		
9	$-X_1$ and b_1 float	-0.3669	1.2199	0.0403										0.9924	0.0726
	$-X_1$ and b_1 = 1.000	-1.3329	1.0000	------										.9580	.1594
	$-X_1, X_2$, and b_1 float	.5015	1.2122	.0300	-1182	-5 406	-22 610	2077	8 690					.9964	.0537
	$-X_1, X_2$, and b_1 = 1.000	-.1898	1.000	------	a-1498	c-6 852	-28 670	5845	24 460					.9667	.1519
30	$-X_1$ and b_1 float	-0.6081	1.1098	0.0474										0.9514	0.1366
	X_1 and b_1 = 1.000	-1.0815	1.0000	------										.9421	.1465
	X_1, X_2, X_3, and b_1 float	-1.1911	1.1073	.0481	c439.4	2 009	8 406	2978	12 460	c0.2777	0.2971			.9542	.1376
	X_1, X_2, X_3, and b_1 = 1.000	-1.7605	1.000	------	c607.7	2 779	11 630	3171	13 270	c.2481	.3183			.9427	.1476
7	$-X_1$ and b_1 float	-0.8368	1.0130	0.0919										0.9604	0.1159
	X_1 and b_1 = 1.000	-.8893	1.000	------										.9603	.1060
	$-X_1, X_2$, and b_1 float	2.0929	1.0914	.0268	-3156	-14 430	-60 380	1768	7 397					.9978	.0308
	$-X_1, X_2$, and b_1 = 1.000	1.3116	1.000	------	-2664	-12 184	-50 980	2951	12 350					.9910	.0553
46	$-X_1$ and b_1 float	-0.4238	1.1576	0.0477										0.9304	0.1753
	X_1 and b_1 = 1.000	-1.1015	1.000	------										.9131	.1937
	X_1, X_2, X_3, X_4, and b_1 float	-4.898	1.1288	.0346	c-365.4	-1 671	-6 991	2213	9 260	0.2999	0.0571	0.5528	0.0570	.9670	.1251
	X_1, X_2, X_3, X_4, and b_1 = 1.000	-1.1820	1.000	------	c-197.8	-905	-3 787	2516	10 530	.3071	.0652	.5335	.0648	.9559	.1429
	X_1, X_3, X_4, and b_1 float	-.7788	1.1263	.0347						.2921	.0565	.5334	.0522	.9665	.1244
	X_1, X_3, X_4, and b_1 = 1.000	-1.3326	1.000	------						.3028	.0634	.5226	.0585	.9558	.1414

[a] $E_a = b_2 \times 1.986 \times 2.303$ calories or $b_2 \times 1.986 \times 2.303 \times 4.184$ J.

[b] Standard deviation of regression response surface.

[c] Dropped, insignificant to a probability level of 0.95.

Because the value of b_1 in each case was close to unity (table V), the equation was recalculated with this slope forced to unity. The error was increased only slightly as measured by the standard error of estimate. The fraction of explained variation is also high in all the three cases, which verifies the validity of equation (5) as a good first approximation.

If all the data for the three plots (46 data points) are combined and run in the same model (eq. (4)), the fit is poorer, and the error correspondingly higher (table V).

Multiple Linear Regression Analysis to Isolate Effects of Flux, Temperature, Zirconium Content and/or Other Variables

Because there was a larger degree of unexplained variation when all the data points were combined in equation (5), it seemed reasonable to assume that there were other factors that significantly affected the total variation. Temperature and zirconium concentration seemed the most obvious, although it appeared the cold-wall induction heated rates were higher than the corresponding tests run in the hot-wall furnace. These other factors along with flux could be evaluated by Multiple Linear Regression Analysis (ref. 20) with a suitable computer program. (The program used for this study was the Multiple Linear Regression FORTRAN IV Program, RAPIER written by S. Sidik, B. Henry, and R. Lambird of Lewis).

With this technique an equation for a response surface can be estimated which unmixes the various factors. This occurs because the coefficients are derived from partial differential equations where the partial derivative of the total variation is taken with respect to one factor while all others are held constant, hence, the term partial regression coefficients. In so doing, the degree of fit, scatter, and the partial regression coefficients for various groupings of the rate data can be analyzed.

The following model equation was used:

$$y = a + b_1 X_1 + b_2 X_2 + b_3 X_3 + b_4 X_4 \tag{6}$$

where

$$y = \log \overline{R}_i$$

$$X_1 = \log \text{flux}$$

$$X_2 = 1/T_2$$

$$X_3 = \text{wt \% Zr}$$

and

$$X_4 = 0 \text{ or } 1$$

This equation represents the effects of flux, temperature, percent zirconium, and a fourth factor X_4, which is a dummy variable used to represent whether the tests were induction heated ($X_4 = +1$) or otherwise ($X_4 = 0$). The last factor, if it is significant, merely shows how much higher the rate is in the cold-wall case. When the data are broken into smaller groups just representing pure columbium and one type of heating, then the equation reduces to just the first two variables.

In the final analysis all 46 rate constants could be combined as a single equation. The flux coefficient b_1 was numerically close to one and was forced to unity with only a slight increase in error.

Table V lists the constants for both b_1 floating and b_1 forced to unity. The regression program is designed so that each of the coefficients is given a statistical test of significance to a given probability level. For example, we can be at least 95 percent sure that any factor we choose to keep is a real, not just a random effect. In this study a 95-percent level was used, and any coefficient testing less than this was automatically dropped and the equation was recalculated. In the 46-point calculation temperature was dropped on this basis. This insignificance can also be inferred qualitatively if the ratio of a coefficient to its deviation is small. The final estimative equation was

$$\log \overline{R}_i = -1.3326 + 1.000 \log \text{flux} + 0.3028 \text{ percent Zr} + 0.2163 X_4 \qquad (7)$$

This equation explains over 95 percent of the total variation with a standard error of estimate of 0.1414.

The sticking probabilities listed in table IV were derived from this final equation. Any given flux can be substituted into the equation to estimate its corresponding reaction rate $\overline{R}_i$. The standard error of estimate is added or subtracted before the antilog is taken to get the upper and lower limits of $\overline{R}_i$. These values divided by the corresponding flux give the sticking probabilities. These equations estimate most precisely over the levels investigated. Extrapolations are usually questionable unless theoretical considerations warrant them. For example, there should be no lower theoretical limit on flux, but extrapolations to 5 percent zirconium would be questionable. Also, tests at higher or lower temperatures might well give significantly different rates.

Comparison with Other Investigations

Other investigators who have run absorption-rate studies on columbium or other works from which such rate constants can be derived from the early stages of low-pressure oxidation studies are Hurlen, et al. (ref. 2), Inouye (ref. 3), Spruiell and Harms (ref. 4), Pasternak and Evans (ref. 10), Kofstad and Espevik (ref. 5), and Delgrosso, et al. (refs. 6 and 7). The columbium - 1 percent-zirconium alloy was studied by Hogan, et al. (ref. 8). These data cover a wide range of oxygen pressures from 10^{-7} to 10^{-2} torr. For our purposes, these pressure values were converted to oxygen fluxes using equation (5) after using the transpiration correction (eq. (B1) on their pressure estimates. The temperature at station one T_1 was assumed in all cases to be 298 K. Figure 7 shows the linear rate absorption constants plotted against flux for all the reference values, as well as the data from this investigation.

Because so many points were involved, the 30 points from figure 5 in this investigation were represented by their unforced regression line. The data of reference 7, made up of 67 data points, were also plotted in this manner. Here, two lines were used to represent the two extreme temperatures (1143 and 1478 K) because temperature did significantly change the rates.

The temperatures indicated on the plot varied from 1123 to 1478 K. Delgrosso and Hogan ran all their tests with an induction heater so these can be considered cold-wall tests. Pasternak used a columbium ribbon heated by self-resistance which also can be considered a cold-wall test. The remainder were hot-wall tests, except for our specimen 88.

Considering the wide ranges of temperature and pressure covered, most of the data seem to agree fairly well, particularly for pure columbium. There does appear to be a change of slope for the pure columbium data from near unity at the low fluxes to near 0.6 at fluxes near 10^{-3} grams per square centimeter per hour, and higher. The effect of temperature is large in the case of the reference 7 data, perhaps because of the larger temperature span. The most puzzling aspect of this plot are the high values Hogan found in his columbium - 1-percent zirconium runs. These would give ϵ's approaching unity. His rates are probably accurate because they were obtained with a microbalance. His oxygen pressure estimates could be low due to the pumping action of the metal chamber walls. In all other cited data, the test rigs were constructed of either glass, quartz, or ceramic. A narrow tubulation to an ionization gage with a significant pumping rate could also be a factor.

In general, figure 7 shows that the sticking probabilities for the cold-wall runs were higher than the hot-wall runs. Also zirconium additions gave higher sticking probabilities. In summary, the literature data show the same general trends as our data except for a more pronounced temperature effect.
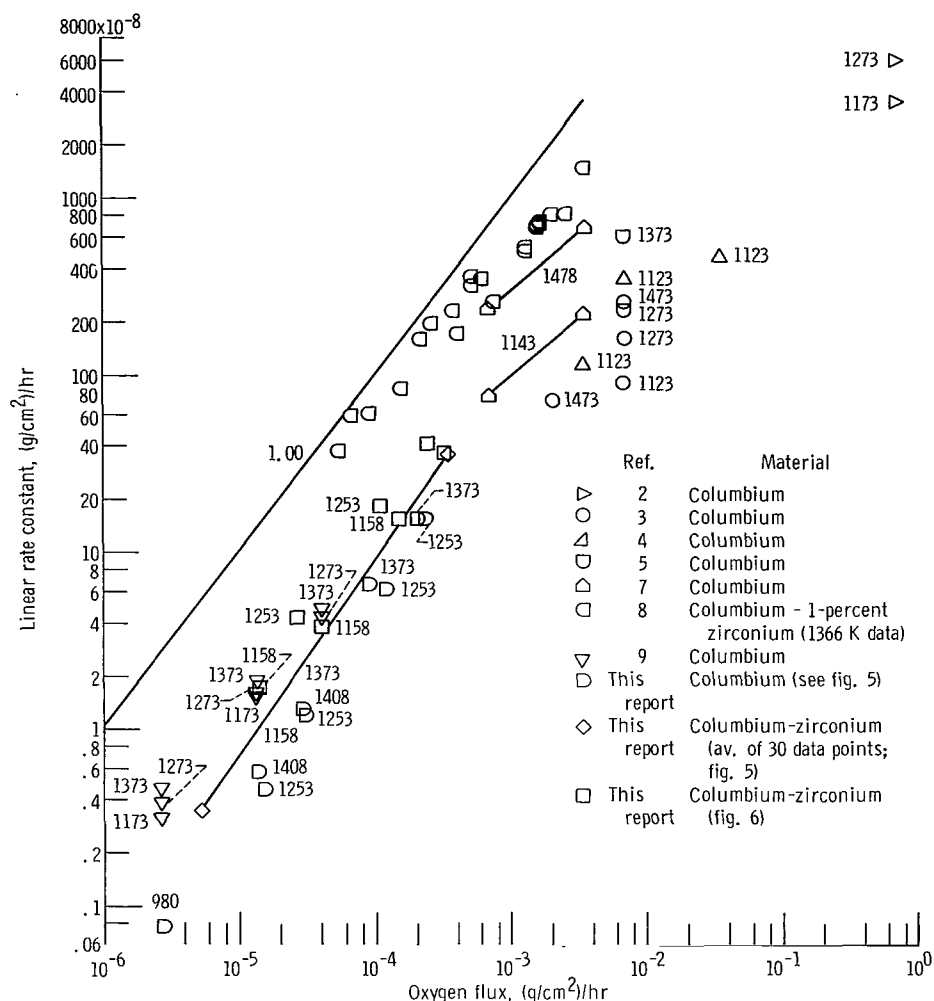
Figure 7. – Linear oxygen absorption rates for columbium and dilute columbium-zirconium alloys for various investigations as function of estimated oxygen flux and specimen temperature. (Includes individual data points and regression line fit of many data points. Numbers with each data point are specimen temperatures in K.

Linear rate constant, $(g/cm^2)/hr$

Oxygen flux, $(g/cm^2)/hr$

	Ref.	Material
▷	2	Columbium
○	3	Columbium
◁	4	Columbium
▽	5	Columbium
△	7	Columbium
◁	8	Columbium – 1-percent zirconium (1366 K data)
▽	9	Columbium
D	This report	Columbium (see fig. 5)
◇	This report	Columbium-zirconium (av. of 30 data points; fig. 5)
☐	This report	Columbium-zirconium (fig. 6)

DISCUSSION

Mechanism of Oxidation

Characteristics of the low-pressure oxidation of columbium and the nominal columbium - 1-percent-zirconium alloy at elevated temperatures have been described by Kofstad and Espevik (ref. 5), Barrett and Rosenblum (ref. 13), Pasternak (ref. 9), Inouye (ref. 3), and others in their low-pressure oxidation studies on columbium. The kinetics that they found can be divided into three main stages: (1) an initial linear rate stage, (2) a subsequent stage with a decreasing oxidation rate, and (3) a final stage characterized by an increasing rate of oxidation.

23

The initial linear stage is due to the solution of oxygen after chemisorption (i.e., adsorption) on the surface. Here, the rate controlling step is the oxygen flux on the metal surface which is primarily a function of the oxygen pressure, provided the metal temperature is high enough so that diffusion into the metal is essentially instantaneous. If the oxygen diffusion rate is high enough, the metal surface is effectively clean (i.e., coverage is low).

Stage 2 commences when the diffusion rate can no longer keep up with the adsorption rate. This occurs almost instantaneously at high pressures unless the specimen is quite thick. The solubility limit is then reached and surface oxidation (stage 3) commences.

In our investigation the test pressures were low enough so that, for the temperatures, thicknesses, and times investigated, the intitial linear rate stage was always maintained. The rate curves for all the steps in table II were similar to those in figure 3 which is typical of stage I oxidation. The linear rate constants derived for each step should, if surface adsorption is rate controlling, be directly proportional to oxygen pressure or more precisely to oxygen flux. Figures 4, 5, and 6 show that, indeed, the linear rate constants are directly proportional to oxygen flux. These plots and regression analyses, however, also show that there is no strong temperature dependence for our data, at least between 1158 and 1373 K.

Pasternak gives the most plausible explanation of the independence of the sticking probability on temperature (ref. 9). The rate of absorption is strictly a function of the arrival rate of the oxygen (i.e., flux) and the number of dual sites available on the surface. The molecules are chemisorbed and diffusion of atomic oxygen follows. No significant physisorption takes place at the test temperatures involved. Activated desorption is apparently not involved.

It can be inferred from calculations that the chemisorbed oxygen diffuses into the metal much faster at low pressures than it arrives both for pure columbium and columbium-zirconium alloys, based on the activation energy for diffusion at these relatively high test temperatures. Thus, for these tests the metal surface is always effectively clean (i.e., coverage is low). Under these conditions, no significant activation energy is involved and the sticking probability is constant.

Two questions which have yet to be resolved are (1) why small amounts of zirconium significantly raise the sticking probability when alloyed to columbium and (2) why cold-wall runs can show up to twice the sticking probability of the hot-wall runs? At this time, no explanation can be given for the zirconium effect; a possible explanation of the second question is suggested as follows:

Four different investigators ran cold-wall tests (fig. 7). They were Pasternak and Delgrosso for pure columbium and Hogan and this investigation for columbium - 1-percent zirconium (sample 88 in this study). In all three investigations, which used

induction heating, the sticking probabilities were much higher than for the hot-wall case. In the remaining cold-wall series of tests, Pasternak used self-resistance heating of the columbium and here the sticking probabilities were also somewhat higher than those derived for the hot-wall case.

The reasons for these differences in the hot-wall and cold-wall sticking probabilities are not known. This whole experimental technique is an averaging process for the oxygen molecules in the system. It would seem that the individual behavior of the molecules would be critical as to how the electronic levels of the oxygen atoms are involved in the adsorption process.

An observation made by Fleming (private communication to the author by R. B. Fleming, General Electric Co., Research and Development Center, Schenectady, N.Y., October, 1965) was that sticking probabilities can be expected to drop as the kinetic energy (i.e., temperature) of the colliding molecules increases. He suggests that a factor of 2 or 3 difference in kinetic energy between room-temperature molecules and 1273 K molecules is not unreasonable. The exact relation would depend on the exact temperature of the furnace walls and specimen, the location and number of molecular collisons before absorption, and the accommodation coefficients for oxygen on hot quartz and hot columbium.

Limitations of Use of Sticking Probabilities – End of Stage I Oxidation

As long as surface adsorption is the rate determining step, sticking probabilities can be used to estimate oxygen contamination of getter metals like columbium. This implies that the rate of diffusion of oxygen into the metal is faster than the effective arrival rate ($\epsilon \times$ flux) of oxygen to the metal surface. This can easily be verified from jump-frequency calculations based on the activation energies of the diffusion of oxygen into the alloy, (ref. 9).

This surface flux would be expected to be rate controlling until the oxygen concentration at the metal surface exceeds the solubility limit for oxygen in columbium at the temperature of interest. At this point surface scaling begins and stage I oxidation (absorption) ends.

When a constant surface flux process is rate controlling, the solution of Fick's diffusion differential equations for the proper boundary conditions gives the following equation (ref. 21):

$$C - C_i = \frac{F}{D}\left[\frac{Dt}{\ell^2} + \frac{3y^2 - \ell^2}{6^2} - \frac{2}{\pi^2}\sum_{n=1}^{\infty}\frac{-1^n}{n^2}\, e^{-Dn^2\pi^2 t/\ell^2}\cos\frac{n\pi y}{\ell}\right] \tag{8}$$

For values of $Dt/l^2 > 1$ the series term is negligible and the equation reduces to

$$C - C_i = \frac{F\epsilon}{D} \left(\frac{Dt}{l^2} + \frac{3y^2 - l^2}{6} \right) \tag{9}$$

where C_i is the initial concentration, C is the concentration at anytime t, $F\epsilon$ is the effective (i. e. , flux $\times$ ϵ) surface flux, D is the diffusion coefficient, t is the time, l is the distance from the surface to the center of the specimen, and y is any point meas- red from the center.

This is the nonsteady-state diffusion case and predicts relatively shallow oxygen concentration gradients. The gradient depends only on Dt/l^2. For example, for pure columbium at 1253 K with $l = 0.038$ centimeter (0.015 in.) and $t = 1$ hour, this ratio equals 1.039 and gives a $C_{y=l}/C_{y=0}$ of 1.53. For $t = 10$ this Dt/l^2 ratio is 10.39, which gives a concentration ratio of approximately 1.04. In our tests for the total specimen exposure time, Dt/l^2 was always much greater than one, indicating a shallow gradient.

Microhardness traverses across the specimens showed near constant hardness through the specimens, which indicates a lack of gradient. Removal of surface layers by grinding and oxygen analysis of the remainder also indicated no apparent gradient.

Under this condition the surface concentration of oxygen will rise gradually from the initial bulk oxygen concentration. The gradient will keep the same shape as the surface concentration rises until this concentration reaches C_s the solubility limit for the formation of columbium monoxide at a given temperature. When $C_{y=l} = C_s$, surface oxide will start to form. Until this time, the process will be characterized by the rate relations described previously: shallow oxygen concentration gradients and no detectable surface oxides. Apparently the surface coverage is low even close to C_s. This is true even in the nominal columbium - 1-percent-zirconium alloys where the initial saturation of the zirconium as zirconium monoxide or zirconium dioxide causes no apparent change in the oxidation kinetics. Columbium oxide surface film formation is again critical.

Once the surface oxide is sufficiently thick, it is assumed the constant surface flux will no longer be rate controlling. Here, the process will become controlled by diffu- sion through the growing oxide and will be proportional to the square root of time (i. e. , parabolic).

If this hypothesis is correct, it should be possible, for a given temperature and thickness of material, to predict when the change of kinetics from a linear to a parabolic rate will occur. Equation (9) can be rewritten with time as the dependent variable as follows:

$$t_s = \frac{(C_s - C_i)}{F\epsilon} - \frac{l^2}{3D} \tag{10}$$

where t_s is time for saturation, F is the flux, and C_s is the solubility limit for columbium monoxide at $y = l$, C_i is the initial oxygen concentration, and ϵ is the sticking probability for pure columbium. Beyond this t_s limit, different sticking probabilities involving the surface oxide would apply, although they would probably not be rate controlling.

The validity of this t_s estimate was verified experimentally for a pure columbium sample (see appendix C).

Thus, when a getter alloy like columbium is exposed at elevated temperatures to oxygen in the molecular flow regime, the oxygen sticking probability is the critical material constant in predicting oxygen contamination.

SUMMARY OF RESULTS AND CONCLUSIONS

The investigation of absorption rate sticking probabilities for oxygen on columbium and dilute columbium-zirconium alloys yielded the following conclusions:

1. The derived low-pressure steady-state sticking probabilities (ratio of absorption rate to flux) between 1158 and 1373 K for oxygen on pure columbium and the columbium - 1 percent zirconium alloy are 0.047 and 0.093, respectively. These results are for conditions when the temperature of the colliding oxygen molecules is nearly the same as for the specimen (i.e., hot-wall case).

2. Under comparable test conditions, but with the temperature of the colliding oxygen molecules relatively low compared with the 1158 to 1373 K specimen, the sticking probability is 0.077 for pure columbium and 0.15 for columbium - 1 percent zirconium (i.e., cold-wall case).

3. The reaction rate data indicate that surface oxygen adsorption is the rate controlling process giving linear absorption rates with time and oxygen flux, and no significant activation energy. The linear rate constant increases with increasing zirconium content and for a given oxygen flux tends to increase with decreasing kinetic energy of the oxygen molecules.

4. A multiple linear regression analysis of the oxygen absorption rate data showed that the following estimating equation can be used:

$$\log R_i = -1.3326 + 1.000 \log \text{flux} + 0.3028 \text{ wt } \% \text{ Zr} + 0.2163 X_4$$

where $\overline{R}_i$ is the linear absorption rate, flux is the oxygen flux, Zr is the zirconium content in the columbium base alloy, and X_4 is the factor which indicates whether the specimen is surrounded by a cold wall (+1) or a hot wall (0). The equation explains over 95 percent of the total variability with a standard error of estimate of 0.1414.

5. The rate and sticking probability estimates are only valid when the oxygen surface flux is rate controlling. This is no longer rate controlling when the solubility limit of oxygen in the alloy is exceeded on the specimen surface forming columbium monoxide. The time to reach this value t_s can be predicted from

$$t_s = \frac{(C_s - C_i)}{F\epsilon} - \frac{l^2}{3D}$$

where C_s is the solubility limit of oxygen in the alloy when columbium monoxide is formed, C_i is the initial oxygen concentration, F is the oxygen flux, ϵ is the sticking probability of oxygen on the alloy, l is one-half the specimen thickness, and D is the oxygen diffusion coefficient.

APPENDIX A

SYMBOLS

A   specimen area, cm^2

C   concentration of oxygen in alloy at any time t, g/cm^3

C_i initial concentration of oxygen, g/cm^3

C_o molecular flow conductance, liters/sec

C_s oxygen saturation limit, g/cm^3

D   oxygen diffusion coefficient in alloy, cm^2/hr

D_i inside diameter of test section, cm

F   oxygen flux, $(g/cm^2)/hr$

F_ϵ effective oxygen flux ($\epsilon \times$ oxygen flux)

$\sigma \overline{R}_i$ standard deviation of $\overline{R}_i$ over test interval

K   conversion factor from (torr)(liters)/sec to g/hr, $= (M/T_0) \times 57.729$

L   distance from P_1 to leading edge of specimen, cm

L_i lengths of i test section, cm

l 1/2 thickness of specimen, cm

M   molecular weight of reacting gas, g

$m\overline{R}_i$ coefficient of variation, $\sigma \overline{R}_i / \overline{R}_i$

P_0 oxygen pressure at ionization gage station 0, torr

P_1 oxygen pressure ionization gage at ionization gage station 1, torr

P_2 estimated average oxygen pressure over specimen

P_3 oxygen pressure at ionization gage station 3, torr

Q_i volumetric pumping rate, (torr)(liter)/sec

$\overline{R}_i$ average oxygen pickup rate over test interval, $(g/cm^2)/hr$

T_0 temperature at station 0, K

T_1 temperature at station 1, K

$T_2(G)$ estimated temperature of the colliding oxygen molecules, K

$T_2(s)$ temperature at test specimen, K

t	time, hr
W_p/A	accumulative weight gain over the test interval, g/cm^2
ΔW_p	total specimen weight gain, g
y	any distance along thickness, t, cm
ϵ	oxygen sticking probability (rate/flux)

APPENDIX B

PROBLEMS ASSOCIATED WITH ESTIMATING OXYGEN FLUX OVER SPECIMEN

The flux over the specimen was estimated by equation (3) as $F = 209.8 \, \overline{P}_2 \sqrt{M/T_{2(G)}}$. This depends on the accuracy of estimating $\overline{P}_2$ and T_2. Because it was not feasible to measure this pressure directly with a gage, it was determined from (1) the downstream gage P_3 and (2) the upstream gage P_1. The downstream P_3 oxygen pressure corrected for temperature (i.e., the transpiration correction) is (ref. 1)

$$\overline{P}_{3-2} = \overline{P}_3 \sqrt{\frac{T_{2(G)}}{T_3}} \tag{B-1}$$

where P_3 is the downstream oxygen pressure, $T_{2(G)}$ is the absolute temperature around the specimen, T_3 is the absolute temperature at P_3 and $\overline{P}_{3-2}$ is the estimated oxygen pressure at the downstream end of the sample. The uncertainty of this estimate was 0.05. The second estimate from P_1 is more complicated because it not only involves a transpiration correction from the cool zone to the furnace zone, but also a pressure drop due to the pumping action of the specimen and the conductance drop between P_1 and the beginning of the specimen. This upstream pressure is (ref. 12)

$$\overline{P}_{1-2} = \overline{P}_1 - \left(\frac{Q_i L_1 M^{1/2} T_1^{1/2}}{3.81 \, D_1^3 T_0}\right)\left(\frac{T_{2(G)}}{T_1}\right)^{1/2} - \frac{Q_i T_{2(G)}^{1/2} M^{1/2}}{3.81 \, T_0} \sum_{i=2}^{3} \frac{L_i}{D_i^3} \tag{B-2}$$

where the first term is the pressure drop in the borosilicate glass tube just after P_I times the transpiration correction on entering the hot section. The second term represents the additional pressure drop through the various diameter quartz sections to the leading edge of the specimen. The L_1 and D_1 are the length and diameter, respectively, of the borosilicate glass tube. The L_i and D_i are the length and diameter of the ith quartz segment, the flow rate Q_i equals $(P_0 - P_1)C_0$, and T_0, T_1, and $T_{2(G)}$ are the temperatures in various test sections. The total length L from P_1 to the leading edge of the specimen is also tabulated for each run. All these values are listed in table VI. The overall uncertainty of this estimate, assuming the validity of the equation, is about 11 percent, based on the uncertainties due to P_1, Q_i, and D. The derived values of $\overline{P}_{3-2}$ and $\overline{P}_{1-2}$ are tabulated in table II for the dimensions and temperatures involved for the various specimen runs. If the two pressures ($\overline{P}_{3-2}$ and $\overline{P}_{1-2}$) are equal, then there is no measurable pressure drop across the specimen. In this study

TABLE VI. – PARAMETERS TO ESTIMATE $\bar{P}_{1-2}$ FOR OXYGEN (M = 32)

Specimen	Oxygen pressure at station 1, $\bar{P}_1$, torr	Volumetric pumping rate, $\bar{Q}_i$, (torr)(liter)/sec	Station 0, T_0	Station 1, T_1	Oxygen molecule, $T_2(G)$	First segment Length, L_1	First segment Diameter, D_1	Second segment Length, L_2	Second segment Diameter, D_2	Third segment Length, L_3	Third segment Diameter, D_3	Total Length of ith quartz segment, L, cm
3	4.79×10^{-5}	1.12×10^{-4}	296	296	1200	7.62	2.20	15.38	2.13	0	0	23.00
36	1.65×10^{-6}	5.32×10^{-6}	296	296	1253	7.62	2.20	14.27	2.13	0	0	21.89
	1.35×10^{-5}	3.54×10^{-5}			1253							
	1.59×10^{-6}	4.75×10^{-6}			1373							
	1.53×10^{-5}	4.65×10^{-5}										
	6.35×10^{-6}	2.24×10^{-5}										
	5.85×10^{-7}	1.70×10^{-6}										
37	8.56×10^{-7}	2.55×10^{-6}	296	296	1253	7.62	2.20	14.27	2.13	0	0	21.89
	1.05×10^{-6}	4.73×10^{-6}										
	3.61×10^{-6}	1.34×10^{-5}										
	8.14×10^{-6}	2.77×10^{-5}										
	1.23×10^{-5}	4.78×10^{-5}										
	3.38×10^{-5}	1.28×10^{-4}						15.88				23.50
50	1.36×10^{-6}	4.58×10^{-6}	296	296	1253	7.62	2.20	16.58	2.13	0	0	24.20
	1.75×10^{-6}	6.00×10^{-6}			1373							
	1.32×10^{-5}	4.27×10^{-5}			1373							
	1.31×10^{-5}	4.21×10^{-5}			1253							
51	9.39×10^{-8}	2.50×10^{-7}	311	311	1253	6.35	3.10	22.42	2.13	0	0	28.77
52	6.15×10^{-7}	1.77×10^{-6}	296	296	1408	7.62	2.20	15.88	2.13	0	0	23.50
	1.41×10^{-6}	4.00×10^{-6}			1408							
	5.87×10^{-6}	2.03×10^{-5}			1373							
	1.38×10^{-5}	4.74×10^{-5}			1373							
	5.67×10^{-7}	1.41×10^{-6}			1253							
	1.29×10^{-6}	3.63×10^{-6}										
	6.13×10^{-6}	1.89×10^{-5}										
	1.42×10^{-5}	4.71×10^{-5}										
59	1.37×10^{-6}	4.46×10^{-6}	324	324	1373	10.0	3.13	14.0	2.99	4.10	3.18	28.10
	1.39×10^{-6}	4.11×10^{-6}	324	324	1373	10.0	3.13	14.0	2.99	4.10	3.18	28.10
61	1.17×10^{-6}	8.29×10^{-6}	324	324	1158	10.0	3.13	14.0	2.99	4.10	3.18	28.10
	1.23×10^{-6}	8.44×10^{-6}			1253							
	1.20×10^{-6}	8.40×10^{-6}			1373							
	1.44×10^{-5}	1.27×10^{-4}			1373							
	1.36×10^{-5}	1.07×10^{-4}			1253							
	1.41×10^{-5}	1.01×10^{-4}			1158							
88	1.63×10^{-5}	1.34×10^{-4}	298	298	298	10.0	3.13	14.0	2.99	11.10	3.18	35.10
	7.33×10^{-6}	5.86×10^{-5}										
	1.67×10^{-6}	1.36×10^{-5}										
	7.62×10^{-7}	5.59×10^{-6}										
	1.57×10^{-5}	1.18×10^{-4}										
	7.06×10^{-6}	5.03×10^{-5}										
	1.74×10^{-6}	1.24×10^{-5}										

\# see errata sheet

$\overline{P}_{1-2}$ was always significantly greater than $\overline{P}_{3-2}$, which implies a pressure drop along the specimen. According to Fleming (ref. 11) this drop is exponential in nature. Therefore, to estimate the average pressure over the specimen, the logs of $\overline{P}_{3-2}$ and $\overline{P}_{1-2}$ are averaged and its antilog estimates $\overline{P}_2$ are used in equation (3). (In the earlier work (ref. 13), there was no P_3 gage, so a pressure drop was not accounted for in the flux calculation. Instead, oxygen flux over the specimen was simply

$$\text{Flux} = 209.88 \, P_1 \left(\frac{T_{2(G)}}{T_1} \frac{M}{T_{2(G)}} \right)^{1/2}$$

These gave biased high flux values and corresponding biased low sticking probabilities. (Introduction of the P_3 downstream gage introduced the whole problem of pressure drop to and across the specimen as well as indicating extraneous gases over the specimen.)

Obviously, the closer the $\overline{P}_{1-2}$ and P_{3-2} are to their estimates, the more confidence in the $\overline{P}_2$ estimate. The ratios varied from 1.09 to 8.90 for columbium-zirconium alloys with an average of 3.36. For pure columbium the ratio of $\overline{P}_{1-2}$ / $\overline{P}_{3-2}$ varies from 1.47 to 2.05 with an average of 1.60. This drop is a function of the diameter of the test section, the length of the specimen, and its sticking probability.

Vacuum fusion analysis for oxygen of 0.635 centimeter long segments along the specimen length also indicate an oxygen pressure gradient along the specimen. This gradient could be inferred from these values, except for oxygen diffusion along the specimen as well, which would tend to flatten the gradient.

These derived average fluxes are listed in table II for each interval. The estimated uncertainty in deriving $\overline{P}_2$ and, hence, the flux is about 13 percent based on the uncertainties in determining $\overline{P}_{3-2}$ and $\overline{P}_{1-2}$. The validity of the flux equation depends on the validity of the transpiration correction which is used in both equations (B1) and (B2).

The transpiration correction applies strictly to the molecular flow regime when the Knudsen number Kn is quite large (>10), and a state of equilibrium exists as defined by Knudsen as zero net mass transfer across a plane rather than an equality of pressure (ref. 22). In our study the Knudsen number was quite high ranging from 50 to 500 but, because of the pumping action of the specimen, Knudsen's equality of flux is only an approximation.

Another problem in using equation (3) is in using the proper temperature $T_{2(G)}$. This is really a measure of the temperature (i.e., kinetic energy) of the oxygen molecules colliding with the specimen surface. The oxygen molecules enter the system at a temperature T_1 and presumably collide at least once with the chamber wall before

striking the specimen. If the accommodation coefficient[1] is unity, one collision is sufficient in the hot-wall case to raise the temperature to $T_{2(G)}$. The cold-wall case is more complicated because the molecule is bouncing back and forth between a hot specimen and the colder wall, but it always strikes the specimen with the energy of the wall, approximately T_1 in our case.

It is more likely that the accommodation coefficients are not unity, however, so it appears the oxygen molecules striking the specimen surface are always at some intermediate temperature, probably much lower in the cold-wall case than in the hot-wall case.

Another complicating factor was in estimating P_3 in equation (B1) because of the presence of extraneous gases detected at this gage by the mass spectrometer. These gases were primarily carbon monoxide and carbon dioxide, but water vapor, helium and hydrogen were also present. These gases were found in increasing amounts with decreasing pressures (refs. 11 and 12). This was not so serious a problem at P_1, which was usually at least a decade higher than P_3. This showed up as an upward bias from a straight line in a P_1 against P_3 log-log plot. No bias was apparent at a $P_1 > 3 \times 10^{-7}$ torr. Values less than this that were unbiased indicated at least 85 percent oxygen at the P_3 gage. On this basis all data with values of $P_1 < 3 \times 10^{-7}$ torr were discarded unless a mass spectrometer at P_3 indicated at least 85 percent O_2. The data points in this grouping with percent oxygen estimates at the P_3 gage were corrected by multiplying the derived flux by the percentage of oxygen present. A regression analysis performed on this corrected data indicated no significant difference in the fit or in the regression constants for this data from the same data uncorrected for oxygen. Thus, for the 46 data points used, no percent oxygen correction was considered necessary. Attempts to correct the biased data for extraneous gases were not successful.

The source of carbon-monoxide and carbon dioxide is in the reaction of oxygen with carbon in the refractory-alloy specimen and gage filaments. Helium diffuses through the hot quartz while H_2O comes off the glass and quartz walls. Hydrogen is outgassed by the hot specimen and is a reaction product of water with the specimen.

---

[1]$\alpha = (T_{2(G)} - T_1)/(T_{2(G)} - T_1)$ where α is the accommodation coefficient ranging from 0 to one, $T_{2(G)}$ and T_1 are the specimen, and P_1 is the temperature and $T_{2(G)}$ is the temperature of the oxygen molecules after colliding with the hot wall or specimen.

APPENDIX C

EXPERIMENTAL VERIFICATION OF PREDICTED END OF STAGE I OXIDATION

The time when oxygen absorption is no longer rate controlling can be predicted from

$$t_s = \frac{(C_s - C_i)}{F_\epsilon} - \frac{l^2}{3D} \qquad (10)$$

where t_s is the time for surface saturation of oxygen in columbium, l is half the thickness, C_s is the solubility limit of oxygen in the metal gms at some temperature T, C_i is the initial concentration of oxygen in the metal, D is the diffusion coefficient of oxygen in the metal at T, and F_ϵ is the effective oxygen flux, gms.

Because both oxygen diffusion rates and solubility limits are available for pure columbium as a function of temperature, it is possible to choose a combination of test temperature and oxygen pressure where a change from a surface-flux controlled reaction to a surface-oxidation controlled reaction should occur say within a 236-hour test run.

Such a test was performed on a pure columbium sample 0.114-centimeter thick ($l \times 0.057$ cm) at 927° C (sample 3 in tables I and II). The C_i was 0.0092 percent with a C_s calculated to be 0.315 weight percent at 927° C (ref. 23). The value of D used was 2.80×10^{-7} square centimeter per second (ref. 24) and converted to square centimeters per hour. Because pure columbium has an value of ϵ of 0.047, it was estimated that an approximate test pressure of 3×10^{-5} torr oxygen would cause C_s to be exceeded within a 236-hour test run, so a break could be detected. Figure 8 shows the accumulated weight gain plot against time on a log-log plot of this special run. A change in mechanism would show up as change in slope from one to one-half. It was calculated that this break should occur at close to $t_s = 26$ hours. The actual P_2 test pressure was estimated to be 3.19×10^{-5} torr. In this run there was no gage present at P_3 so the estimated flux was derived strictly from P_{1-2} and the P_{1-2}/P_{3-2} ratios for the other pure columbium tests.

There is an apparent break in the curve somewhere between 20 and 100 hours but it is not as sharp as expected. This is partly because, as the rate started to slow down, the pressure at P_1 started to build up, thus, it was difficult to hold P_1 constant. During the test P_1 rose from 4.71 to 6.00×10^{-5} torr. This compared with the straight linear runs where the P_1 could be held quite constant with a coefficient of variation less than 10 percent.

The initial break from a linear rate is close to 20 hours. From 20 to 100 hours there is an intermediate rate characterized by a patchy buildup of surface oxide. The terminal behavior appears parabolic.
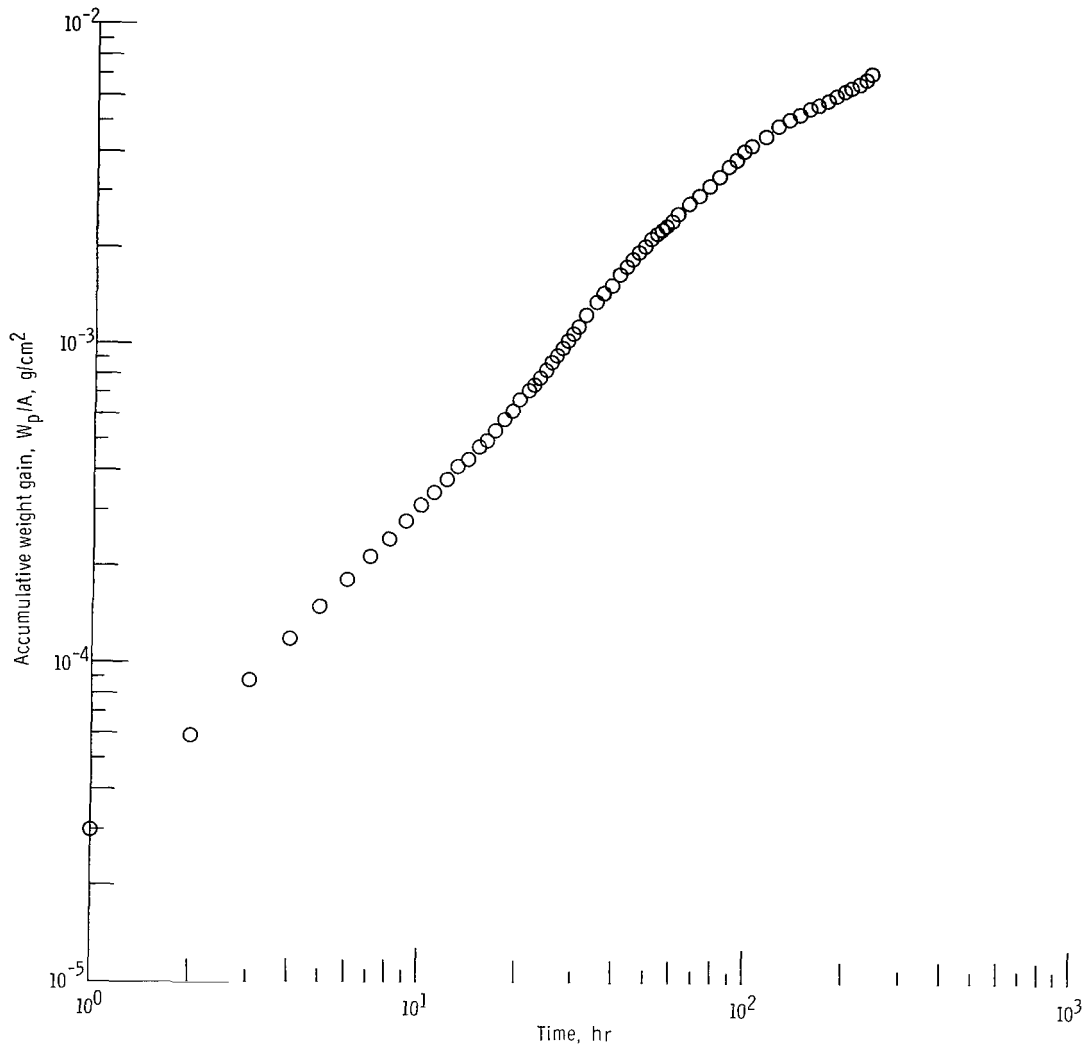
Figure 8. - Oxygen weight gain for pure columbium (0.114 cm thick) as function of time at 1300 K and in 10^{-5} torr oxygen pressure range. Curve shows weight gain to be linear with time until 20 hours. After 100 hours behavior appears parabolic. Initial break point can be estimated from equation (10).

When the uncertainties in diffusion coefficients, solubilities, and flux determinations are considered, it was thought that the agreement with the calculated value of 26 hours is good. This break to a parabolic rate was further confirmed by a tight sooty black oxide completely covering the specimen showing that surface oxidation did, indeed, take place. The scale was shown by X-ray diffraction to be predominantly columbium dioxide with a trace of columbium pentoxide. The oxygen concentration gradient was also apparently quite shallow through the specimen as indicated by the Knoop microhardness traverses. This implies the bulk concentration was close to C_s throughout as was expected when process ϵ is initially rate controlling.

36

REFERENCES

1. Dushman, S.; and Lafferty, J. M.: Scientific Foundations of Vacuum Technique. Second ed., John Wiley & Sons, Inc., 1962.

2. Hurlen, Tor; Kjöllesdal, Hallstein; Markali, Joar; and Norman, Nico: Oxidation of Niobium. Tech. (Scientific) Note No. 1, Central Institute for Industrial Research, Oslo, Norway, Apr. 1959.

3. Inouye, H.: The Oxidation of Columbium at Low Oxidation Pressures. Columbium Metallurgy. Interscience Publ., 1961, pp. 649-665.

4. Spruiell, J. E.; and Harms, W. O.: The Oxidation of Columbium at 850° C in Oxygen at Low Pressures. Univ. Tennessee, Dept. Chem. Met. Eng., 1960.

5. Kofstad, Per; and Espevik, Svein: Low-Pressure Oxidation of Niobium at 1200° to 1700° C. J. Electrochem. Soc., vol. 112, no. 2, Feb. 1965, pp. 153-160.

6. Harrison, R. W.; and Delgrosso, E. J.: An Apparatus for Gravimetric Determination of the Effects of Low Pressure Oxidation. J. Sci. Instr., vol. 41, Apr. 1964, pp. 222-224.

7. Delgrosso, E. J.; Carta, J. S.; and Ricard, A.: The Low Pressure Oxidation of Pure Columbium. Rep. PWAC-460, Pratt and Whitney Aircraft, Sept. 1965.

8. Hogan, J. F.; Limoncelli, E. A.; and Cleary, R. E.: Reaction Rate of Columbium-1 Zirconium Alloy with Oxygen at Low Pressures. Rep. TIM-901, Pratt and Whitney Aircraft, Aug. 24, 1965.

9. Pasternak, R. A.: High-Temperature Oxidation and Nitradation of Niobium in Ultrahigh Vacuum. Rep. SRIA-132, Stanford Research Inst., Nov. 15, 1964.

10. Pasternak, R. A.; and Evans, B.: Adsorption, Absorption, and Degassing in the Oxygen-Niobium System at Very Low Pressure. J. Electrochem. Soc., vol. 114, no. 5, May 1967, pp. 452-457.

11. Fleming, R. B.: Contamination Exposures of Columbium and Cb-1Zr Alloy Specimens. Rep. DMS-65-2, General Electric Co. (NASA CR-72264), Jan. 22, 1965.

12. Fleming, R. B.: Contamination Exposures of Columbium and Tantalum Alloy Specimens. General Electric Co. (NASA CR-54934), July 15, 1966.

13. Barrett, C. A.; and Rosenblum, L.: Oxygen "Pumping Efficiency" of Refractory Metals. Proceedings of the NASA-AEC Liquid-Metals Corrosion Meeting, Vol. 1. NASA SP-41, 1964, pp. 307-312.

14. Wagener, S.: A Method for Measuring the Efficiency of Getters at Low Pressures. British J. Appl. Phys., vol. 1, Sept. 1950, pp. 225-231.

15. della Porta, P.: Performance Characteristics of Barium Getters with Particular Reference to Their Application in Thermionic Values. Vacuum, vol. 4, no. 3, July 1954, pp. 284-302.

16. della Porta, P.: Apparatus and Techniques for Measurements of the Adsorption of Gases by Evaporated Getters. Vacuum, vol. 10, no. 1/2, Feb./Apr. 1960, pp. 181-187.

17. Orr, W. H.: Use of the Flow-Method to Study the Kinetics of Gases on Clean Surfaces. National Symposium on Vacuum Technology, Transactions. American Vacuum Soc., 1962, pp. 484-490.

18. Santeler, Donald J.; Holkeboer, David H.; Jones, Donald W.; and Pagano, Frank: Vacuum Technology and Space Simulation. NASA SP-105, 1966.

19. Hickam, C. William: Corrosion Product of the Tantalum-Interstitial Oxygen-Potassium System at 1800° F (1255° K). NASA TN D-4213, 1967.

20. Draper, Norman; and Smith, H.: Applied Regression Analysis. John Wiley & Sons, Inc., 1966.

21. Crank, J.: The Mathematics of Diffusion. Oxford University Press, 1956, p. 58.

22. Arney, G. D., Jr.: and Bailey, A. B.: Effect of Temperature on Pressure Measurements. AIAA J., vol. 1, no. 12, Dec. 1963, pp. 2863-2864.

23. Gebhardt, Erich; and Rothenbacher, Rolf: Investigation of the Niobium-Oxygen System. II. Solution of Oxygen in Niobium and Precipitation of Oxide from Supersaturated Mixed Crystals. Z. Metallk., vol. 54, Nov. 1963, pp. 623-630.

24. Bunn, Patricia M.; Cummings, D. G.; and Leavenworth, H. W., Jr.: The Effect of Zirconium on Internal Friction in Columbium. J. Appl. Phys., vol. 33, no. 10, Oct. 1962, pp. 3009-3013.

"The aeronautical and space activities of the United States shall be conducted so as to contribute . . . to the expansion of human knowledge of phenomena in the atmosphere and space. The Administration shall provide for the widest practicable and appropriate dissemination of information concerning its activities and the results thereof."

— NATIONAL AERONAUTICS AND SPACE ACT OF 1958

NASA SCIENTIFIC AND TECHNICAL PUBLICATIONS

TECHNICAL REPORTS: Scientific and technical information considered important, complete, and a lasting contribution to existing knowledge.

TECHNICAL NOTES: Information less broad in scope but nevertheless of importance as a contribution to existing knowledge.

TECHNICAL MEMORANDUMS: Information receiving limited distribution because of preliminary data, security classification, or other reasons.

CONTRACTOR REPORTS: Scientific and technical information generated under a NASA contract or grant and considered an important contribution to existing knowledge.

TECHNICAL TRANSLATIONS: Information published in a foreign language considered to merit NASA distribution in English.

SPECIAL PUBLICATIONS: Information derived from or of value to NASA activities. Publications include conference proceedings, monographs, data compilations, handbooks, sourcebooks, and special bibliographies.

TECHNOLOGY UTILIZATION PUBLICATIONS: Information on technology used by NASA that may be of particular interest in commercial and other non-aerospace applications. Publications include Tech Briefs, Technology Utilization Reports and Notes, and Technology Surveys.

Details on the availability of these publications may be obtained from:

SCIENTIFIC AND TECHNICAL INFORMATION DIVISION

NATIONAL AERONAUTICS AND SPACE ADMINISTRATION
Washington, D.C. 20546